CHAPTER 2

Alternative Refrigerants and Cycles for Compression Refrigeration Systems

2.1 INTRODUCTION

Refrigerant is the substance which is used as working fluid in a thermodynamic cycle, undergoes a phase change from liquid to vapour and produces cooling. These are used in refrigeration, air conditioning, and heat pumping systems. They absorb heat from one area, such as an air conditioned space, and reject it into another, such as outdoors, usually through evaporation and condensation, respectively. These phase changes occur both in absorption and mechanical vapour compression refrigeration systems, but they do not occur in systems operating on a gas cycle using a fluid such as air (ASHRAE Handbook, 1997, Fundamentals, Chapter 18).

The chronological evolution of refrigerants has been shown in Table 2.1 (Radermacher and Hwang, 2005). The first refrigerant used in a continuous refrigeration system by William Cullen in 1755 was water. But the credit for building the first vapour compression refrigeration system goes to Jakob Perkins who used sulphuric (ethyl) ether obtained from India rubber as refrigerant. In the beginning, the goal was to produce refrigeration only; whatever substance gave the desired results was used as refrigerant. All refrigerants were either flammable or toxic at that point in time. In 1930's, Thomas Midgley introduced R-12 (CF_2Cl_2, i.e., Dichlorodifluoromethane) and R-11 ($CFCl_3$, i.e., Trichloromonofluoromethane) as nontoxic and nonflammable refrigerants. This led to developments of a series of CFCs and HCFCs which deemed to be stable, nontoxic, nonflammable, and having a desired boiling point substances. During that period the main objective was safety and durability. The CFCs were not only being used as refrigerant but also as solvent, foam blowing agent, aerosol and in fire extinguishers. Later in 1980s, it was discovered that halogens and CFCs and other related substances react with ozone layer in atmosphere and thin down the ozone layer because of their higher atmospheric lifetime. Halogen, which results from the breakdown of CFCs in atmosphere combines with greenhouse gases and enhances the global warming threat. International consensus was made to stop production and use of halogenated refrigerants for which Montreal Protocol came into existence in 1987. In 1997, Kyoto Protocol was ratified to limit the green house gases causing global warming. Recent attention towards depletion of stratospheric ozone layer and global warming put a question mark to the present use of refrigerant in refrigeration and air conditioning (RAC) industry.

Year	Refrigerant	Chemical Makeup, Formula	First Developer/User
1980s	R123	CF_3CCl_2H	
1980s	R124	CF_3CFClH	
1980s	R125	CF_3CF_2H	
1990s	R134A	CF_3CFH_2	
1990s	R407C	R32/R125/R134a (23/25/52 wt%)	
1990s	R410A	R32/R125 (50/50 wt%)	
1990s	R404A	R125/R143a/R134a (44/52/4 wt%)	
2000s	R417A	R134a/R125/R600 (50/46.6/3.4 wt%)	
	R422A	R134a/R125/R600a (11.5/85.8/3.4 wt%)	
	R423A	R134a/R27ea (52.5/47.5 wt.%)	
	R432A	R1270/ RE170 (80/ 20 wt%)	
	R433A	R1270/R290 (30/70 wt%)	

These protocols initiated the search of alternative refrigerants and cycles, which are not only environment-friendly but also, consist of all desired properties of an ideal refrigerant and cycle. The HCFCs can be utilized as interim solution because of its low Ozone Depletion Potential (ODP) and Global Warming Potential (GWP) compared to CFCs. HCFC-123, HFC-134a can be used in low pressure and medium pressure systems. As no single substance can pass under ODP, GWP, toxicity, flammability, cost and efficiency criteria simultaneously, the search has already been started to find suitable azeotropic and zeotropic blends. These synthesized substances are expected as potential refrigerants in future which can fulfil desired requirements.

2.2 ALTERNATIVE REFRIGERANTS

Before the discovery of ozone hole in early 1970s, the refrigeration and air-conditioning industry was relying heavily on CFCs, HCFCs, Halons (BFCs) and their azeotropics. CFCs contain only chlorine, fluorine and carbon atoms but they cause ozone depletion (ODP of CFCs varies between 0.3 and 1) and have very long atmospheric life time (a few centuries). CFCs which have been in extensive use are R-11, R-12, R113, R114, R115, etc. Halons or BFCs contain bromine, fluorine and carbon atoms. For example, R-13B1 and R12B1 are BFCs. Their ozone depletion potential is very high, for example, ODP of R-13B1 is 10 and it was in use since 1995 for very low temperature vapour compression refrigeration systems. However, after the discovery of ozone hole the era for alternative refrigerants has started.

Further, the alternative refrigerants are classified as:

1. Pure refrigerants (i.e., single component refrigerants)
   (a) Natural refrigerants, i.e., inorganic and organic compounds
   (b) Hydrofluorocarbons (HFCs)
2. Refrigerant mixtures/blends
   (a) Based on the number of pure components, i.e., binary / ternary /quaternary
   (b) Azeotropic /near azeotropic / zeotropic (non-azeotropic)

2.2.1 Pure Refrigerants (Single Component Refrigerants)

Natural refrigerants are those substances which exist in our biosphere, for example, air, water, ammonia (which are inorganic compounds) and hydrocarbons. Natural refrigerants are non-ozone depleting and also have negligible global warming potential. On the other hand, HFCs contain only hydrogen, fluorine, and carbon atoms and cause no ozone depletion but have high global warming potential. HFCs group include R-134a, R-32, R-125, and R-245ca.

2.2.2 Refrigerant Mixtures/Blends (Multi-Component Refrigerants)

(a) Binary/Ternary/Quaternary Refrigerant Mixtures/Blends

Binary mixtures, as the name suggests, consist of two pure refrigerant components mixed in required proportions. For example, R-410A is a binary mixture of R125 and R32 in equal proportions by weight. Similarly, ternary and quaternary mixtures contain three and four pure refrigerants respectively. R-407C is a ternary mixture comprising R-32/ R-134a/ R-125 (23%/52%/25% by weight).

(b) Azeotropic Mixtures/Blends

An azeotropic is a mixture of multiple components (refrigerants) of volatilities that evaporate and condense as a single substance and do not change in volumetric composition or saturation temperature when they evaporate or condense at constant pressure. HFCs azeotropics are blends of refrigerant with HFCs. ASHRAE assigned numbers between 500 and 599 for azeotropes. HFCs azeotrope R-507, a blend of R-125/R-143, is a commonly used refrigerant for low-temperature vapour compression refrigeration systems.

An azeotropic mixture has a temperature-pressure-concentration diagram where the saturated vapour and saturated liquid lines coincide at a range of concentrations, as shown in Fig. 2.2. At the point or region where the saturated vapour and liquid lines merge, the mixture of the two substances behaves with the properties of a single substance, having properties different from either of its constituents.

Even combinations that are azeotropic at certain concentrations at one pressure may not be perfectly azeotropic at another pressure, as shown in Fig. 2.3.

The azeotropic concentration changes as the pressure increases. Usually, the azeotropic region shifts toward the high concentration of the low- temperature boiling refrigerant (material A in this case). Even the azeotrope R-502, which has been used successfully for many years, was subject to fractional distillation at certain operating pressures.

(c) Near Azeotropic and Zeotropic (Non-Azeotropic) Refrigerant Mixture/Blends

A near azeotropic is a mixture of refrigerants whose characteristics are near those of an azeotropic. It is thus named near azeotropic because the change in volumetric composition or saturation

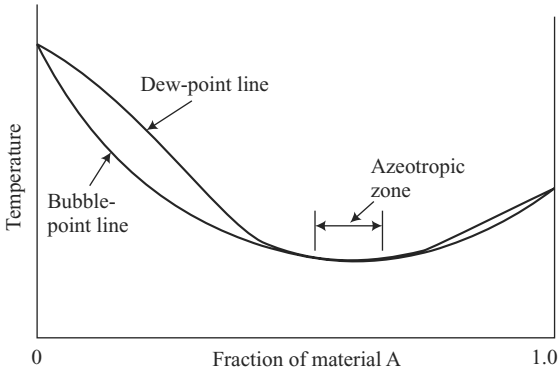

Fig. 2.2 An Azeotropic Mixture of Materials *A* and *B* in the Range of 50-to-60% of A

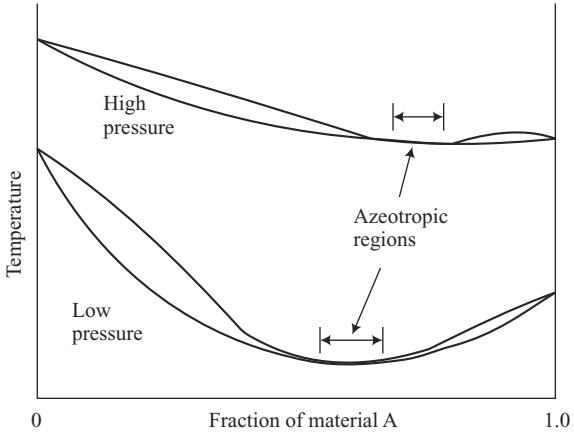

Fig. 2.3 A Shift in the Azeotropic Region as the Pressure Changes

temperature is rather small, such as, 0.5°C to 1.1°C. ASHRAE assigned numbers between 400 and 499 for near azeotropic/zeotropic refrigerant mixtures. R-404A (R-125/R-134a/R-143a) and R-407B (R-32/R-125/R 134a) are HFCs near azeotropic refrigerant mixture (NARM). R-32 is flammable; therefore, its composition is usually less than 30% in the mixture. HFCs near azeotropic refrigerant blends are widely used for vapour compression refrigeration systems.

The diagram of the temperature-pressure-concentration relationship of an ideal zeotropic mixture might appear as shown in Fig. 2.4. In a zeotropic mixture, the concentration of the two substances in the vapour is different from that in the liquid at a given pressure and temperature. There are certain applications where the properties of a zeotrope are advantageous, such as in the autocascade system for ultra low temperatures. For conventional industrial refrigeration systems, however, the

time dependency spreads from 20 to 100 years and written as GWP_{20} (for 20 years), GWP_{100} (100 years lifetime), etc. Emission of one kg of R-134a is roughly equivalent to emission of 1300 kg of CO_2 in 100 years, so GWP_{100} of R-134a is 1300. Thus, the GWP of a greenhouse gas is an index relative to that of CO_2 to trap heat radiated from earth to space.

(c) Total Equivalent Warming Impact (TEWI): It is the factor to evaluate the environmental effect of GHGs in an appliance. TEWI provides the measure of the environmental impact of GHGs from manufacture, operation, service and end of life disposal of the equipment. It takes account of both the emissions of refrigerants and indirect emissions due to energy consumption and fossil fuels used. TEWI combines the effects of direct emissions of refrigerants (and also the foam insulation blowing agents) from appliance during its lifetime with the indirect emission of CO_2 from the combustion of fossil fuels and generation of electricity use by the appliance or the system.

TEWI is defined by the following equation:

$$\text{TEWI} = m_{ref} \,.\, \text{GWP}_{ref} \,.\, Z + m_{ba} \,.\, \text{GWP}_{ba} + \text{t.E.f}$$

where TEWI : Total Equivalent Warming Impact in kg CO_2

m_{ref} = Mass of refrigerant in kg

GWP_{ref} = Global Warming Potential of refrigerant in kg CO_2

Z = Number of charges of refrigerant during service life

m_{ba} = Mass of blowing agent in kg

GWP_{ba} = Global Warming Potential of blowing agent in kg CO_2

t = Service life of appliance in year

E = Annual energy consumption of appliance in kWh/yr

f = CO_2 factor of energy conversion in kg CO_2/kWh_{el}

The first two terms on the right hand side of the TEWI equation are for direct contribution of refrigerants during servicing and blowing agents to global warming and the last term is for the contribution to global warming due to the energy consumed during the lifetime of the appliance. There can be many additional factors to consider, for example, emission during the initial charge and recovery of refrigerants at the end of life of the appliance.

The TEWI can also be expressed as follows (Bitzer Refrigerant Report 16):

$$\text{TEWI} = (\text{GWP} \times L \times n) + (\text{GWP} \times m\,[1 - \alpha_{\text{recovery}}]) + (n \times E_{\text{annual}} \times \beta)$$

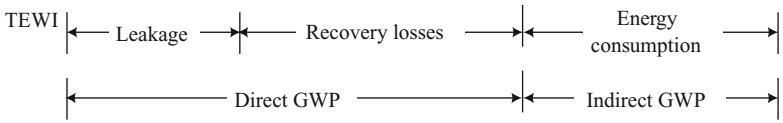

GWP = Global warming potential [CO_2-related]

L = Leakage rate per year [kg]

n = System operating time [Years]

m = Refrigerant charge [kg]

$\alpha_{recovery}$ = Recycling factor

E_{annual} = Energy consumption per year [kWh]

β = CO_2-Emission per kWh [Energy Mix]

		R402B	R125/290/22 (38.0/2.0/60.0)	0.033, 2310			Ice machines
		R403B	R-290/22/218 (5.0/56.0/39.0)	0.031, 4310			Very low temperature single stage refrigeration, it is also a replacement for R13B1
		R408A	R-125/143a/22 (7.0/46.0/47.0)	0.026, 3020		Compatible with mineral oil, Alkylbenzene and polyolester lubricant	Medium* and low** temperature commercial and industrial direct expansion refrigeration systems
Substitutes (Long-term Alternatives)	**HFC**	R134a	Pure	0, 1300	R12, R22$^{\Theta}$	Compatible with polyolester lubricant for stationary equipment and polyalkaline glycol for automotive air conditioning systems	Household appliances, refrigeration (commercial and self-contained equipment), centrifugal chillers and automotive air conditioning
		R152a	Pure	0, 120	Used as part components of blends	N.A.	N.A.
		R125	Pure	0, 3400			
		R143a	Pure	0, 4300			
		R32	Pure	0, 550			
		R227ea (CF_3-CHF-CF_3)	Pure	0, 3500	R12B1, R114$^{\Theta}$	Polyolester oil	Suitable for air conditioning devices functioning in high temperature environments, high temperature heat pumps, and thermal collectors.

Contd...

		R437A	R143a/125/ 134a	0,1680	R12, R500	Compatible with traditional and new lubricants; in most cases no change of lubricant type during retrofit is required.	Automotive air conditioning systems designed for R12 stationary air conditioning systems. Medium temperature stationary refrigeration systems designed for R12, such as supermarket display cases, food storage/processing. It is a service refrigerant and replacement for HCFC blends such as, R401A and R409A.
		R407C	R134a/125/32 (52/25/23)	0, 1650	R22	Polyolester oil	Medium temperature commercial and industrial direct expansion refrigeration and A/C
		R417A	R600/134a/125 (3.4/50.0/46.6)	0, 2240		Mineral, alkyl benzene or fully synthetic lubricants	Commercial refrigeration display cabinets
		R417B	R600/134a/125 (2.75 /18.25/79)	0, 2920		Mineral oil	
		R422D	R125/134a/600a (65.1/13.5/3.4)	0, 2620		Compatible with mineral and alkyl-benzene Oil	Medium and low temperature commercial and industrial direct expansion refrigeration
		R427A	R32/125/143a/134a (15/25/10/50)	0, 2010		Polyolester oil	To replace R-22 in existing equipment for a wide range of temperatures. To retrofit low temperature refrigeration units as well as air conditioning installations. Many industrial installations in commercial refrigeration (supermarkets,etc., in industrial refrigeration

Contd...

2.3.1 Lorenz Cycle

The main assumption of Carnot cycle (single, two or mixed phase) is that the cycle accepts and rejects heat at a constant temperature level throughout the heat absorption and heat rejection process. However, in most applications, heat is supplied by or rejected to a fluid (air, water, brine etc.) whose temperature changes during the heat exchange processes (Fig. 2.5). This leads to the presence of so called *pinch point*, and thus, at points 1 and 4 and at points 6 and 8 the temperature differences between both fluid streams become very small, consequently, the heat transfer rate becomes less. The entropy generation or exergy destruction is also small due to the fact that heat is transferred over a small temperature difference. In contrast, at points 2 and 3 and also for points 5 and 7, the temperature differences are large, the heat transfer rate is more as well and so is the entropy production or exergy destruction.

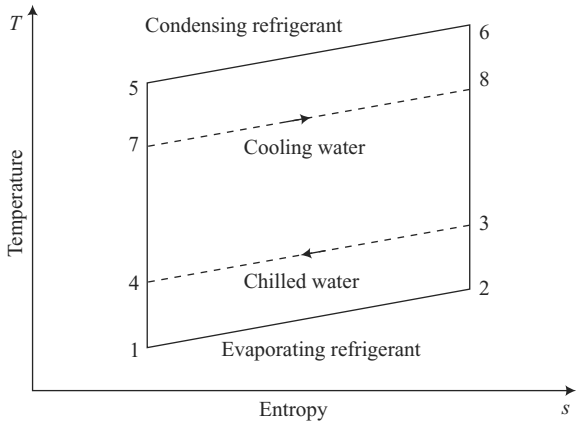

Fig. 2.5 Heat Exchange in Refrigerant Mixture/ Blend and Heat Absorbing and Rejecting Medium

The Lorenz Cycle (Radermacher and Hwang, 2005) addresses this issue. This cycle is for a working fluid that changes its temperature (i.e., it has a temperature glide) during the course of its phase change (evaporation and condensing) (Fig. 2.5). In the ideal case, the change in temperature throughout during both phase change processes matches that of the fluid (heat absorbing or rejecting medium), thus the overall entropy production or exergy destruction reduces significantly and the exergetic efficiency of the cycle improves to the largest possible extent, too. The refrigerant mixtures/ blends have the potential to approach the requirements of the Lorenz cycle depending on the degree to which they match the application glide in both the evaporator and the condenser. It should be noted that even for the same heat exchange area, a Lorenz cycle for the blends that better matches the source and sink glides gives higher cycle efficiency because it operates at an improved mean temperature than the corresponding pure refrigerant.

2.3.2 Transcritical Carbon Dioxide Compression Refrigeration Cycle (Singh, 2009)

In a transcritical carbon dioxide compression refrigeration cycle, the supercritical CO_2 is expanded to a subcritical state. The throttling loss is very large as compared to conventional refrigeration

systems due to the higher pressure change during the expansion. Thus, basic transcritical carbon dioxide refrigeration cycle offers lower efficiencies when compared to HCFCs and HFCs.

In the basic transcritical CO_2 compression refrigeration cycle (Fig. 2.6), the refrigerant vapours coming out of the evaporator (EVA) is compressed using compressor (COM) above the critical conditions (P_{cr} = 73.77 bar and T_{cr} = 31.10°C) and then cooled in a gas cooler (GCO). Then, this cooled gas is throttled in an expansion valve (EXP) and low temperature and low pressure liquid CO_2 enters the evaporator.

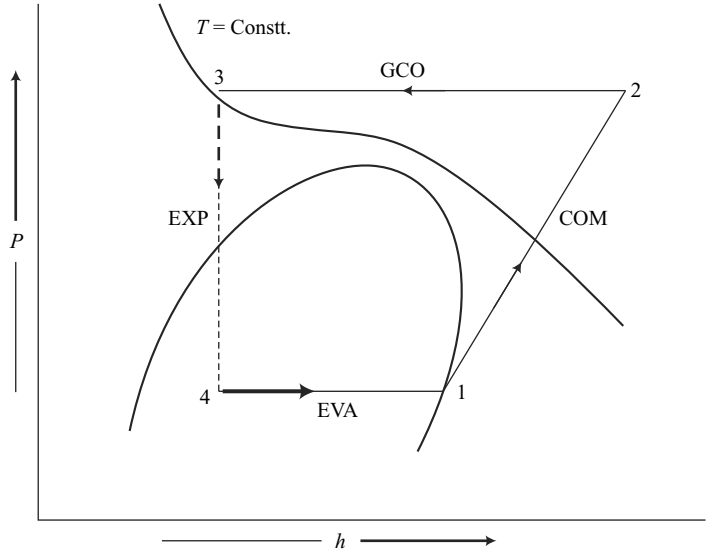

Fig. 2.6 Transcritical Carbon Dioxide Refrigeration Cycle

2.4 THERMODYNAMIC ANALYSIS OF VAPOUR COMPRESSION REFRIGERATION CYCLE WITH ALTERNATIVE REFRIGERANTS

2.4.1 Vapour Compression Refrigeration (VCR) System

Aprea *et al.* (1996) reported that VCR systems are normally used for cold storage and supermarket refrigeration. These systems operate between condensing temperature of 35°C and evaporating ones in the range of (–)40°C to 0°C. The suitable working fluid for these applications is the refrigerant R502 which is an azeotropic mixture of refrigerants HCFC22 and R115. Both of these refrigerants are harmful to ozone layer. The ozone depletion potential for HCFC22 and R115 is 0.055 and 0.4 respectively (Calm and Hourahan, 2001). Aprea *et al.* (1996) experimentally evaluated general characteristics and system performances of substitutes for R502 in a refrigeration plant. They examined R402A, R402B, R403B, R408A, R404A, R407A and FX40. All substitutes showed performances very close to those of R502 except R403B whose COP was found to be about 8% lower than that of R502.

Park *et al.* (2008a, b) experimentally tested the thermodynamic performance of R433A, R432A and HCFC22 in a heat pump bench tester under air conditioning and heat pumping conditions. Both R432A and R433A offer similar vapour pressure to HCFC22 for possible 'drop-in' replacement. The test results showed that the COP of R433A was 4.9-7.6% higher than that of HCFC22 while the capacity of R433A was found to be 1.0-5.5% lower than that of HCFC22 under both test conditions. The COP of R432A was found to be 8.5-8.7% higher than HCFC22 and its refrigerating capacity was 1.9-6.4% higher than that of HCFC22 under both test conditions. The compressor discharge temperatures of R432A and R433A were lower than that of HCFC22. The amount of charge required for both these refrigerants was 50-57% lower than that of HCFC22 due to their low density. Overall, both these refrigerants are good long-term environment-friendly alternatives to replace HCFC22 in residential air conditioners and heat pumps due to their excellent thermodynamic and environmental properties with minor adjustments.

Chen (2008) carried out the performance analysis, using simulation software, of R410A as a long-term alternative refrigerant with zero ODP (ozone-depleting-potential) for replacing HCFC22 in a split-type residential air conditioner. It was deduced that the adoption of R410A could be helpful for air conditioners to decrease their heat exchanger size or improve their operation efficiency for power saving. Moreover, compared to HCFC22, R410A could, in fact, help alleviate its overall impact on global warming through significantly reducing the indirect global warming impact.

Arora *et al.* (2007) carried out the exergy analysis of a vapour compression refrigeration system with HCFC22, R407C and R410A.The results were computed for actual vapour compression cycle without liquid vapour solution heat exchanger. It was concluded that R410A is a better alternative as compared to R407C, with high coefficient of performance and low exergy destruction ratio when considering for refrigeration applications. For air-conditioning applications, R407C is a better alternative than R410A.

Lorentzen (1995), Calm (2008), Wang and Li (2007) and Riffat *et al.* (1997) had advocated the use of natural refrigerants such as ammonia, propane, CO_2, water and air. The fourteenth refrigerant report released by Bitzer International specifies R717 (ammonia), R723 (60% ammonia + 40% dimethyl ether), HC290 (propane) and HC1270 (propylene) as long-term halogen free alternative refrigerants to HCFC22 and R502 (Bitzer International: Refrigerant Report no. 14-Edition A-501-14, 2007). Palm (2008) reported that vapour pressure curves of the propane and propene are quite similar to those of HCFC22 and ammonia, indicating that the application areas would be same. Recently, air conditioning provided by ammonia refrigeration systems has found applications on college campuses and office parks, small-scale buildings such as convenience stores, and larger office buildings. These applications have been achieved by using water chillers, ice thermal storage units, and district cooling systems (http://www.iiar.org//aaranswers_history.cfm?). Pearson (2008) reported that the benefits of using ammonia for water chilling applications have been reported by many authors. Moreover, ammonia is widely used in industrial systems for food refrigeration, cold storage, distribution warehousing and process cooling. It has more recently been proposed for use in applications such as water chilling for air conditioning systems.

Siller *et al.* (2006) have reported that ammonia is not a contributor to ozone depletion, greenhouse effect or global warming. Thus, it is an "environment-friendly" refrigerant. Ammonia has no

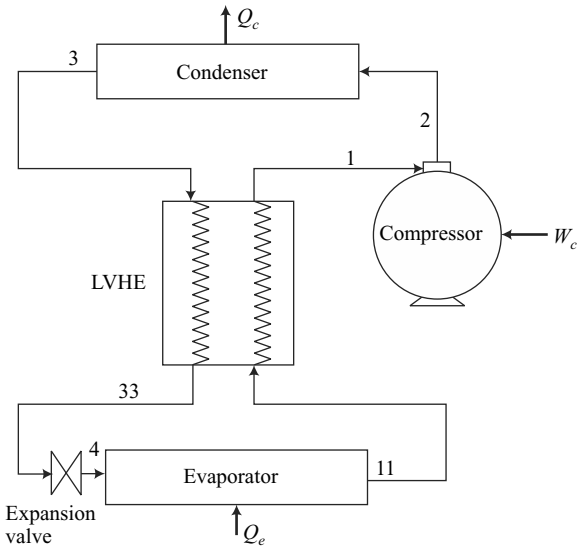

Fig. 2.7 Schematic Diagram of a Vapour Compression Refrigeration System with Liquid Vapour Heat Exchanger (lvhe) (Dincer, 2003)

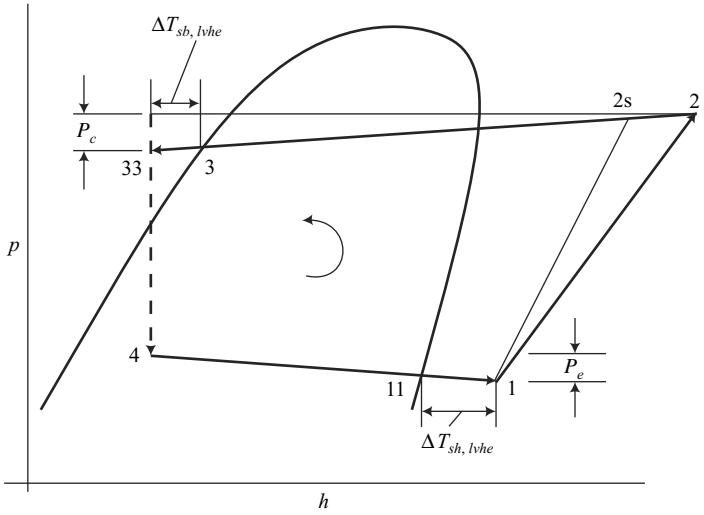

Fig. 2.8 P-h Diagram of VCR System Shown in 2.8(a)

pressure losses in evaporator and condenser. The main components of a vapour compression refrigeration (VCR) system are evaporator, compressor, condenser and a throttling device (expansion valve). A liquid vapour heat exchanger may be incorporated between the liquid line and suction line to transfer the heat from hot liquid refrigerant leaving the condenser to the cold suction vapour entering the compressor. It improves the overall system performance in some cases.

7. The effects of sub-cooling in condenser and superheating in evaporator are neglected.
8. Difference between evaporator and cold room temperature, $(T_r - T_e)$ is taken as 2°C.

Two groups of variations in COP, EDR and exergetic efficiency are plotted. In the first group condensing temperature is varied between 30 and 60°C for a constant evaporating temperature equal to – 40°C. In the second case condenser temperature is taken as –55°C whereas evaporator temperature is varied. The data assumed for plotting Figs. 3.5 to 3.10 is identical as mentioned above except the evaporator and condenser temperatures are (–) 25°C and 55°C respectively.

2.4.1.3 Results and Discussion

Effect of Condenser Temperature

It is observed from Fig. 2.9 (a) and (b) that with increase in condenser temperature, COP of the VCR system reduces. This happens because with the increase in condenser temperature, the dryness fraction of the liquid refrigerant at the exit from expansion device increases and consequently the cooling capacity goes down. Simultaneously, the power consumed by the compressor also increases because of increase in pressure ratio across the compressor and both these factors cause COP to reduce. The COP of R507A is slightly better than R404A. R502 exhibits better COP than both R507A and R404A. The COP for R502 is 3.7% to 25% and 5.7% to 23 % higher in comparison to R507A and R404A respectively. Ammonia and HCFC22 outperform the other three refrigerants. The HCFC22 performs better in comparison to ammonia up to 40°C condensation temperature whereas above 40°C, ammonia gives better COP.

The exergetic efficiency is expressed using equation (2.14). For constant evaporation temperature, only numerator (i.e., COP_{vcr}) changes and denominator (COP_{rr}) remains constant therefore exergetic efficiency is directly proportional to COP of the VCR cycle. Thus, it also reduces, likewise COP, with increase in condenser temperature. The trends of variation in exergetic efficiency are similar to trends of COP curve for these refrigerants. Even the percentage difference in exergetic efficiency of R502 and R507A and R404A are also analogous. Exergy destruction ratio is inversely proportional to exergetic efficiency as expressed in equation (2.19) and hence EDR curves are approximate mirror images of exergetic efficiency curves as depicted in Fig. 2.9 (b).

Effect of Variation in Evaporation Temperature

In the second group (Refer Fig. 2.10 (a), (b) and (c)), the variation of COP, EDR and exergetic efficiency, with evaporating temperature (– 40°C to 0°C) for a constant condensing temperature equal to 55°C, have been plotted. The COP increases with increase in evaporator temperature because of reduction in compressor work and increase in cooling capacity. The COPs of R507A and R404A are lowest among the refrigerants considered. In the ascending order of COPs, the sequence of refrigerants is R404A followed by R507A, R502, R22 and R717. The COP curves of R507A and R404A overlap each other at 55°C condenser temperature. This overlapping of COP curves may not exist at condenser temperatures above or below 55°C because the values of COP obtained at 55°C were identical for – 40°C evaporation temperature also (refer Fig 2.8 (a)). The COP of R502 is approximately 17% higher at –40°C and 10% higher at 0°C in comparison to R507A and R404A.

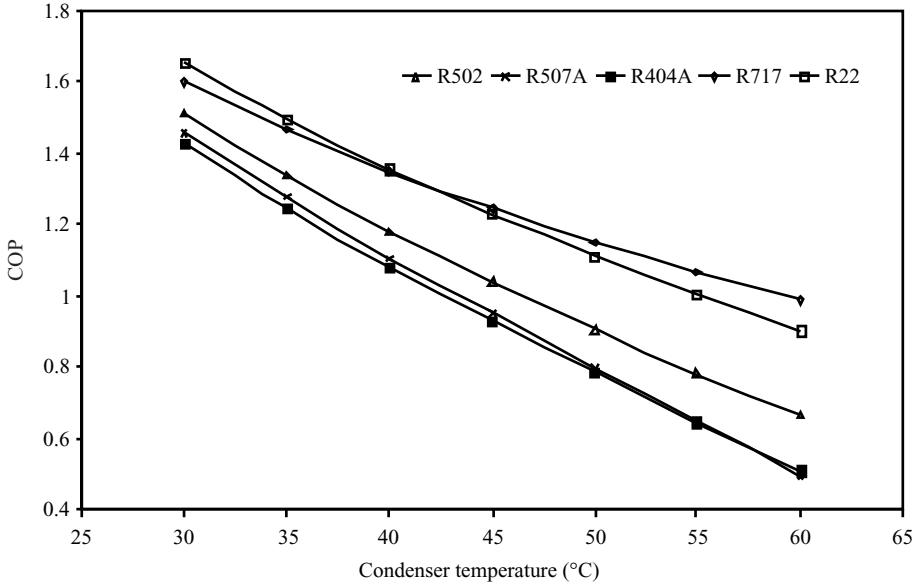

Fig. 2.9(a) Variation of COP versus Condenser Temperature

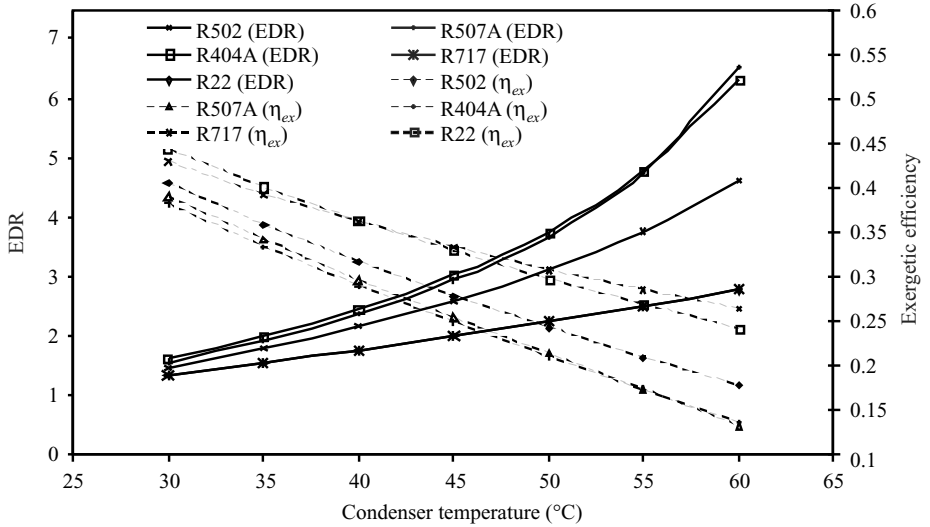

Fig. 2.9(b) Exergetic Efficiency and EDR versus Condenser Temperature

Figure 2.10 (b) and (c) illustrates the variation of EDR and exergetic efficiency with evaporation temperature. The trend of EDR curves is approximate mirror image of exergetic efficiency curves. The reason for such a behaviour has already been explained. Figure 2.10 (c) illustrates the variation of exergetic efficiency with evaporator temperature. The significant feature of Fig. 2.10 (c) is the rise and fall of the exergetic efficiency with increase in evaporation temperature. Such behaviour of

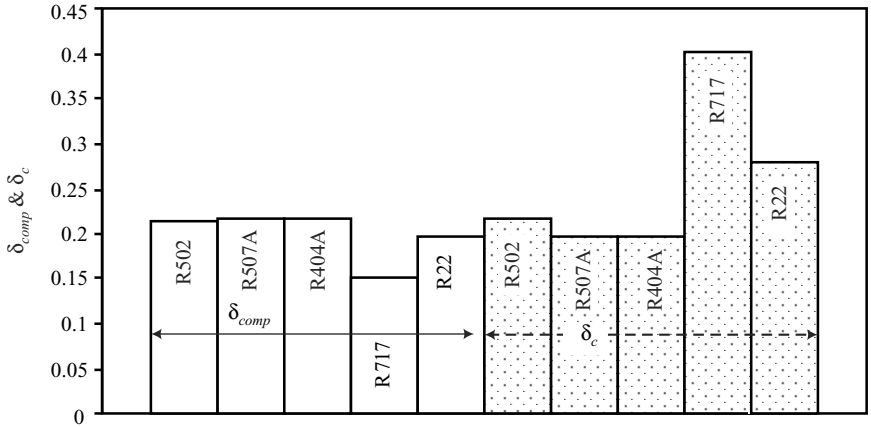

Fig. 2.11(a) Efficiency Defects in Compressor and Condenser for Various Refrigerants

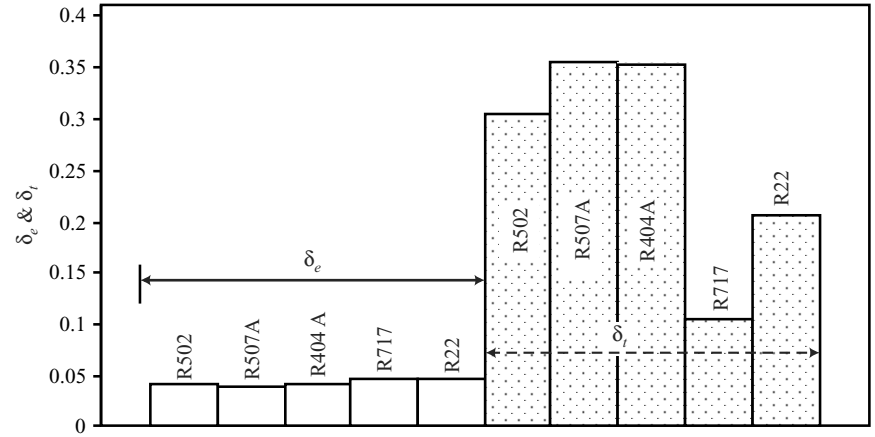

Fig. 2.11(b) Efficiency Defects in Evaporator and Throttle Valve for Various Refrigerants

also increases with increase in degree of sub-cooling. The increase in COP and exergetic efficiency is maximum for R507A among all the refrigerants and lowest for ammonia.

Effect of Superheating in Evaporator

Figure 2.13(a) and (b) illustrates the effect of superheating in evaporator on COP and exergetic efficiency. It is observed that superheating does not have much effect on COP and exergetic efficiency as shown in these figures. In case of R717 there is slight drop in COP and exergetic efficiency. For other refrigerants there is slight increase in COP and exergetic efficiency.

Effect of Effectiveness of Liquid Vapour Heat Exchanger

The effect of variation in effectiveness of liquid vapour heat exchanger on COP and exergetic efficiency is shown in Fig. 2.14 (a) and (b). It is understood that COP and exergetic efficiency increase with increase in effectiveness of 'lvhe'.

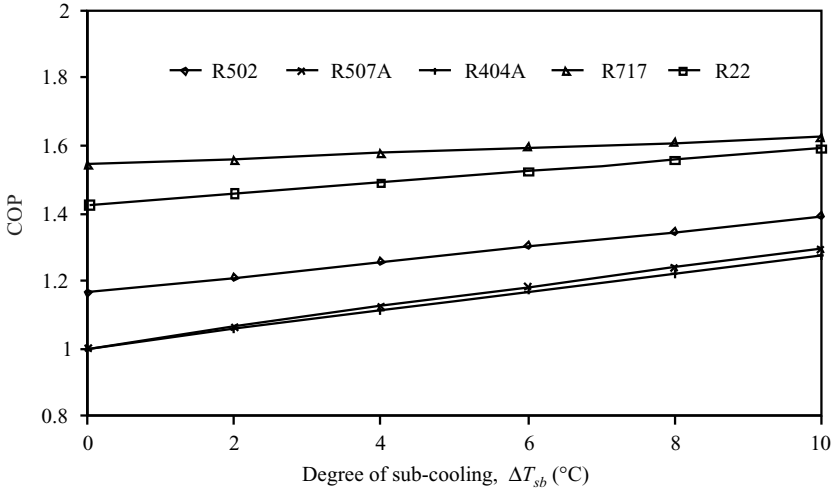

Fig. 2.12(a) Effect of Sub-cooling in Condenser on COP

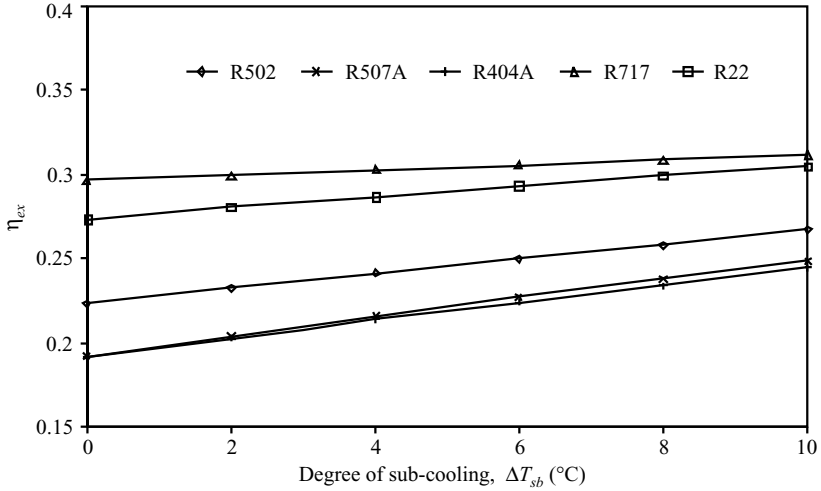

Fig. 2.12(b) Effect of Sub-cooling in Condenser on Exergetic Efficiency

An increase in effectiveness of 'lvhe' from 0 to 1 causes sub-cooling of saturated liquid in 'lvhe' which accounts for increase in the cooling effect. Simultaneously superheating of the suction vapour causes isentropic compression to take place along the isentropic lines having reduced slope thereby increasing the compressor power input. The combined effect of both these factors accounts for increase in the COP of all refrigerants under consideration except ammonia for which COP reduces. The exergetic efficiency of R502, R507A, R404A and HCFC 22 increases whereas it reduces for R717.

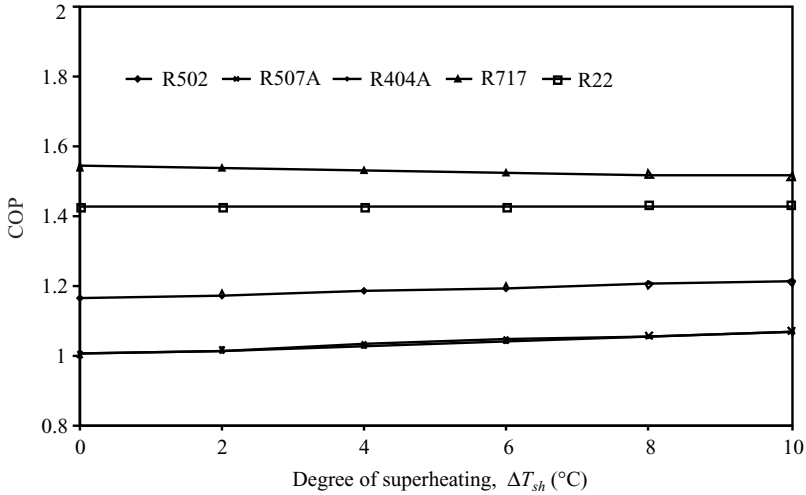

Fig. 2.13(a) Effect of Superheating in Evaporator on COP

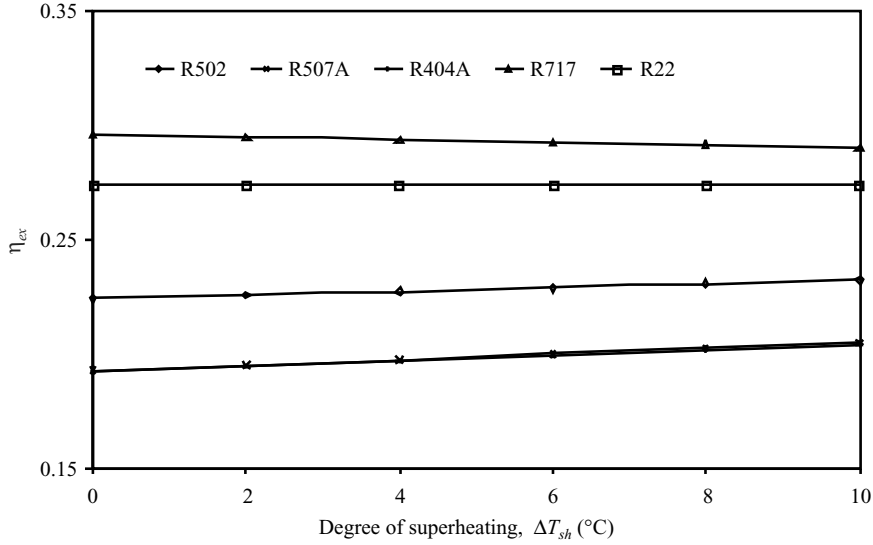

Fig. 2.13(b) Effect of Superheating in Evaporator on Exergetic Efficiency

Effect of Variation in Isentropic Efficiency of Compressor

Figure 2.15(a) and (b) show the effect of variation in compressor efficiency on COP and exergetic efficiency. With increase in isentropic efficiency of compressor, the power required to compress the refrigerant vapour reduces whereas the refrigerating capacity remains constant and the COP increases. The exergetic efficiency being directly proportional to COP (refer equation 2.14) also

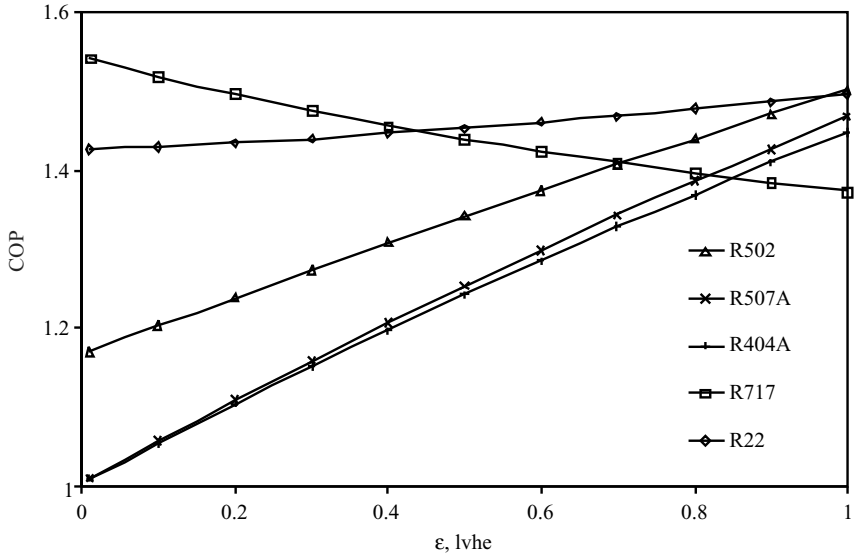

Fig. 2.14(a) Effect of Effectiveness of 'lvhe' on COP

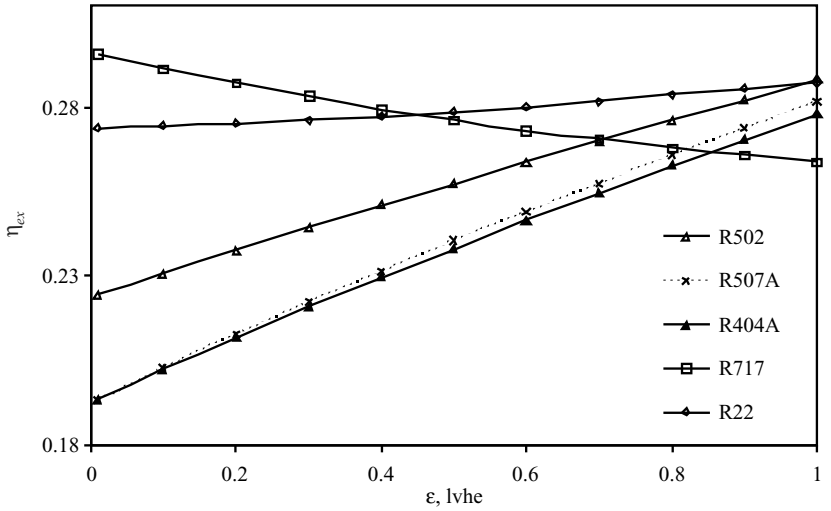

Fig. 2.14(b) Effect of Effectiveness of 'lvhe' on Exergetic Efficiency

increases. The exergy destruction ratio is inversely proportional to the exergetic efficiency, therefore it decreases. The increase in COP and exergetic efficiency with increase in isentropic efficiency is highest for ammonia.

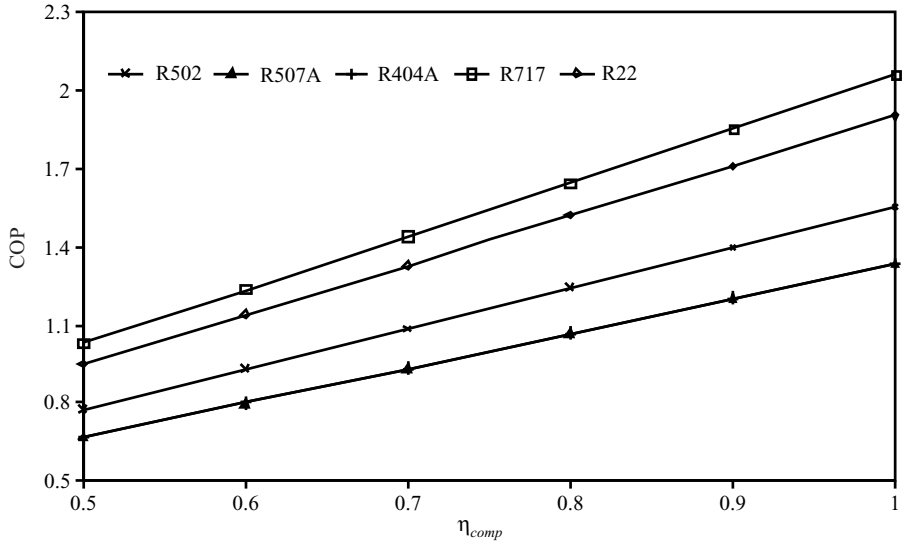

Fig. 2.15(a) Effect of Compressor Efficiency on COP

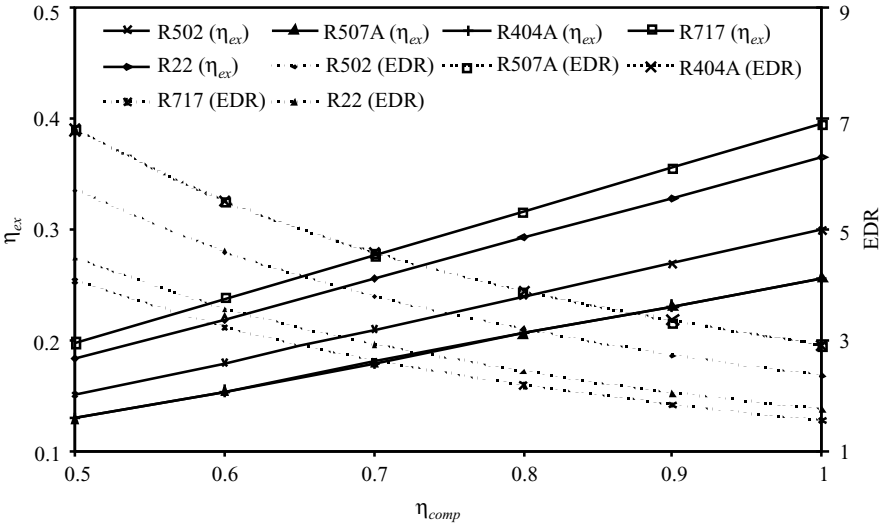

Fig. 2.15(b) Effect of Compressor Efficiency on Exergetic Efficiency and EDR

Effect of Pressure Drops in Evaporator and Condenser

The effects of pressure drops in evaporator and condenser on COP and exergetic efficiency are shown in Fig. 2.16 (a) and 2.16 (b). It is observed that the COP reduces with increase in pressure drop in evaporator. As the pressure drop in evaporator enhances, there is decrease in cooling capacity due to reduction in specific refrigerating effect and pressure ratio across compressor increases

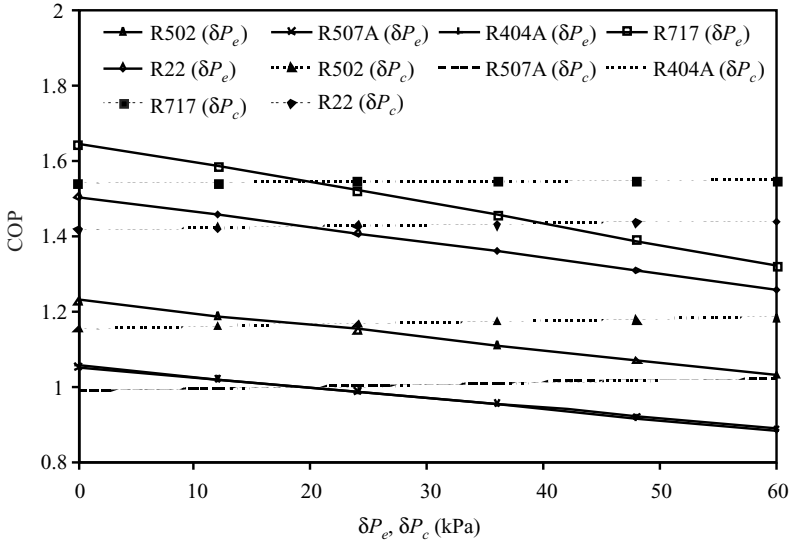

Fig. 2.16(a) Effect of Evaporator and Condenser Pressure Drops on COP

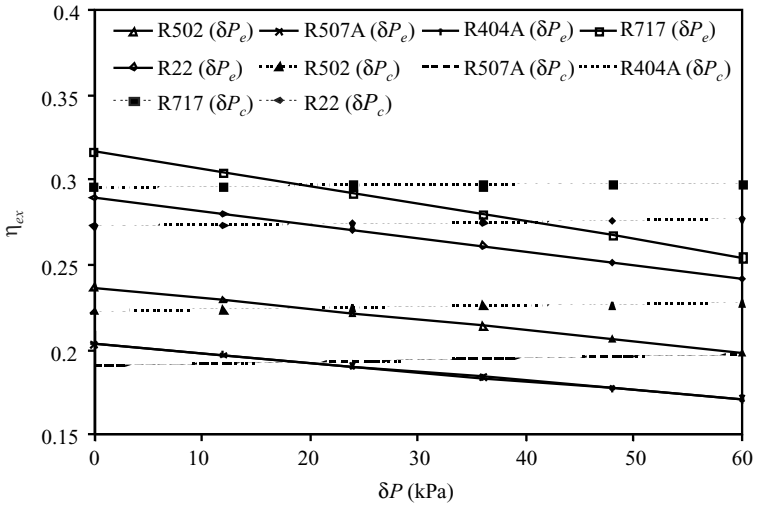

Fig. 2.16(b) Effect of Evaporator and Condenser Pressure Drops on Exergetic Efficiency

causing compressor power to increase. Hence, both COP and exergetic efficiency reduce. The pressure drop in condenser is beneficial since the exit state from expansion device is now nearer to the liquid saturation curve and hence specific refrigerating effect increases for the same specific compressor work. Thus COP and exergetic efficiency increase. The increase in the values of COP and exergetic efficiency is small.

Effect of Performance Parameters on Efficiency Defects in VCR System Components

Table 2.4 shows the effect of sub-cooling, superheating, effectiveness of 'lvhe', isentropic efficiency of compressor and pressure drops in evaporator and condenser on efficiency defects occurring in

	Efficiency defect (δ) and exergetic efficiency (η_{ex})	Base cycle	Sub-cooling by 10 K in condenser ($\Delta T_{sb,c}$)	Superheating by 10 K in evaporator (ΔT_{sh})	Effectiveness of 'lvhe' (ε, *lvhe* = 1)	Isentropic η_{comp} increases from 75% to 80% (i.e. η_{comp}= 80%)	Pressure drop (δPe) in evaporator increases to 60 kPa	Pressure drop (δPc) in condenser increases to 60 kPa
	δ_e	0.04681	0.04757	0.0448	0.03706	0.04991	0.1114	0.04685
	δ_t	0.1045	0.0819	0.09997	0.02596	0.1114	0.09057	0.1027
	δ_{lvhe}	–	–	–	0.01865	–		
	η_{ex}	0.2965	0.31198 (5.22%)	0.29058 (–1.99%)	0.2636 (–11.1%)	0.31619 (6.64%)	0.25412 (–14.29%)	0.29753 (0.35%)
HCFC 22	δ_{comp}	0.1955	0.1955	0.1897	0.1566	0.1576	0.1924	0.1955
	δ_c	0.27765	0.29006	0.29476	0.43976	0.28042	0.26806	0.2793
	δ_e	0.04626	0.04782	0.04394	0.03803	0.04935	0.1113	0.0464
	δ_t	0.2067	0.1616	0.1969	0.04465	0.2205	0.1865	0.2023
	δ_{lvhe}	–	–	–	0.0339	–	–	–
	δ_{ex}	0.2738	0.30502 (11.4%)	0.27465 (0.31%)	0.2871 (4.86%)	0.29212 (6.69%)	0.24179 (–11.69)	0.27651 (0.99%)

the systems components for the refrigerants under consideration. It is observed that providing a liquid vapour heat exchanger is the best option of increasing the exergetic efficiency for R502, R404A and R507A. The increase in the value of exergetic efficiency for HCFC22 is little whereas in case of R717, the exergetic efficiency reduces nearly by 11%. Sub-cooling in the condenser is the second best option to improve the exergetic efficiency of R502, R404A and R507A. The best option to increase the exergetic efficiency of R717 is to improve the isentropic efficiency of compressor. Improving the isentropic efficiency of the compression process by 5% also improves the exergetic efficiency of all other refrigerants by approximately 6.6%. The pressure drop in condenser also account for meager increase in exergetic efficiency by about 1.7%. This is because of reduction in efficiency defect in throttle valve. The superheating in evaporator causes the exergetic efficiency to reduce for R502 and R717 whereas it enhances the exergetic efficiency of R507A, R404A and HCFC22. All other factors lead to reduction in exergetic efficiency. The percentage change in exergetic efficiency is also specified in braces in last row.

2.4.2 Multistage Vapour Compression Refrigeration Systems

Multistage refrigeration systems are usually used for applications which demand very low temperatures which cannot be obtained economically through a single-stage system. According to Dincer (2003), multistage compression refrigeration systems are needed where large temperature and pressure differences exist between the evaporator and the condenser. For VCR systems operating at temperatures below (–)30°C and pressure ratios higher than 6, a multistage VCR system is employed. Some of the disadvantages of the high pressure ratio across compressor are (i) decrease in volumetric efficiency leading to decrease in system capacity and COP (ii) high discharge temperature.

For two-stage VCR cycles, the inter-stage pressure (corresponding to the minimum compressor work) is commonly taken as the geometric mean of the refrigerant condensation and evaporation pressures, which is only applicable for a perfect gas with complete inter-cooling between the stages. However, Threlkeld (1966) demonstrated that for two-stage refrigeration cycles, the optimum inter-stage pressure is much different than the geometric mean pressure. Baumann and Blass (1961) found that optimum occurred at a point quite close to equal pressure ratios in the stages when compressor and motor efficiencies are considered. Goseny (1967) studied the two-stage refrigeration system for various situations; however, he has not given any general expressions for the optimum inter-stage pressure. Keshwani and Rastogi (1968) determined the optimum inter-stage pressure in a two-stage VCR system for refrigerant CFC12. Their research was based on minimization of overall compressor work. Arora and Dhar (1973) used the discrete maximum principle, discussed by Katz (1962), to solve the problem of optimum inter-stage pressure allocation in multistage compression systems for CFC12, with and without inter-cooling between the stages. The results showed that the optimum inter-stage pressure approximately equals the geometric mean of the condensation and evaporation pressures. However, when the flash inter-cooler was incorporated, they found a considerable difference between the geometric mean and the optimal pressure values. Prasad (1981) determined the optimum inter-stage pressure in a two-stage VCR system for the refrigerant CFC12. Their study was based on the maximization of COP. The results revealed that the inter-stage temperature of a two-stage VCR system is given by the geometric mean of the condensation and evaporation temperatures. Zubair and Khan (1995) showed that the optimum

inter-stage pressure for a two-stage refrigeration system can be approximated by the saturation pressure corresponding to the arithmetic mean of the condensation and evaporation temperatures. Zubair *et al.* (1996) found that optimum inter-stage pressure for refrigerant HFC134a for maximum COP of the system was close to the saturation pressure corresponding to the arithmetic mean of the refrigerant condensation and evaporation temperatures. The analysis was performed for evaporator temperature (–)30°C, condenser temperatures ranging between 40 and 70°C, compressor efficiency 65%, sub-cooling equal to 3°C and pressure drops in condenser, evaporator and suction line equal to 5%. It was also shown that the system irreversible losses are lowest at an intermediate saturation temperature near to arithmetic mean of the condensation and evaporation temperatures. Nikoladis and Probert (1998) used the exergy analysis to examine the behaviour of two-stage compound compression-cycle, with flash inter-cooling, using refrigerant HCFC22. The condensation and the evaporation saturation-temperatures were varied from 298 to 308K and 238 to 228K respectively. They concluded that greater the temperature difference between condenser and the environment or the evaporator and the cold room, the higher is the irreversibility rate. However, they did not compute the optimum inter-stage temperature (pressure) based on exergy analysis method. Ratts and Brown (2000) computed the optimum reduced intermediate temperature for HFC134a in a two-stage VCR system using entropy generation minimization method. It was revealed that this method gives better results than geometric mean method for evaluation of inter-stage temperature. Ouadha *et al.* (2005) investigated a two-stage VCR system using propane and ammonia and optimized inter-stage pressure for maximization of exergetic efficiency. It was shown that the optimum inter-stage pressure was very close to the saturation pressure corresponding to the arithmetical mean of the refrigerant condensation and evaporation temperatures. Their results were valid for the evaporator temperature of –30°C, condenser temperatures ranging between 30 and 60°C and compressor efficiency equal to 80%. However, they did not consider the effects of sub-cooling, superheating and pressure drops in system components for computing the optimum inter-stage temperature (pressure).

2.4.2.1 Description of Two-stage Vapour Compression Refrigeration (VCR) System

Figure 2.17(a) and (b) shows the schematic and ln *P-h* diagram for a two-stage VCR cycle. The main components of the cycle include low-pressure (LP) compressor, flash inter-cooler, high-pressure (HP) compressor, condenser, expansion valves and evaporator. The refrigerant from the suction line at state 1 is compressed by the LP compressor to the flash inter-cooler, which is operating at an inter-stage pressure. The separated vapour, due to throttling (during the processes 5-6) and de-superheating of the compressed vapour at state 2, yields the increased mass of vapour entering the HP compressor at state 3. The high-pressure superheated vapour leaves the HP compressor at state 4 and enters the condenser. The vapour is condensed in the condenser at state 5 before being throttled to the flash inter-cooler pressure at state 6. The saturated liquid after the flash inter-cooler at state 7 enters the expansion valve, where it expands to the evaporator pressure. At state 8 it leaves the expansion valve and enters the evaporator. In the evaporator, it receives heat from the refrigerated space.

2.4.2.2 Thermodynamic Analysis of the Two-stage VCR Cycle

The thermodynamic analysis of the two-stage VCR system involves the application of principles of mass conservation, energy conservation and exergy balance.

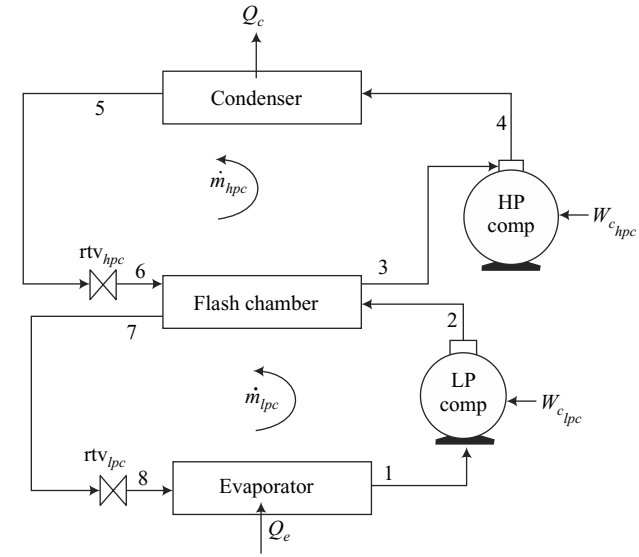

(a)

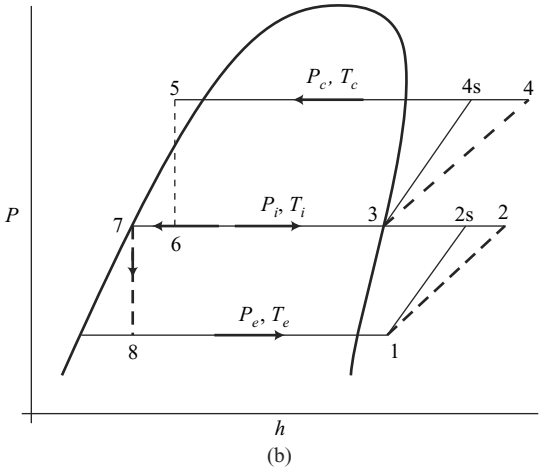

(b)

Fig. 2.17(a) Schematic Diagram of a Two-stage VCR System
(b) ln P-h Diagram of Two-stage System Represented in Fig. 2.17 (a)

Mass Balance

The mass flow rates through the LP and HP stages are $\dot{m}_{lpc}$ are $\dot{m}_{hpc}$ respectively.

Energy Balance of two-stage system

The energy balance of a two-stage VCR cycle allows the computation of mass flow rates through LP and HP stages and heat and work transfer rates through various components.

Energy balance across evaporator

The energy balance across evaporator allows determining of mass flow rate in LP stage. The refrigerant mass flow rate (in kg s^{-1}) through the evaporator for $\dot{Q}_e$ kW of refrigeration capacity is given by

$$\dot{m}_{lpc} = \dot{Q}_e / (h_1 - h_8) \tag{2.20}$$

Energy balance across flash chamber

The energy balance across flash chamber allows computing the mass flow rate in the HP stage. The energy balance across flash chamber is specified through equation (2.21)

$$\dot{m}_{lpc}(h_2 - h_7) = \dot{m}_{hpc}(h_3 - h_6) \tag{2.21}$$

COP of two-stage VCR system is given by equation (2.22)

$$\text{COP}_{ts} = \frac{\dot{Q}_e}{\dot{W}_{comp_{lpc}} + \dot{W}_{comp_{hpc}}} = \frac{\dot{m}_{lpc}(h_1 - h_8)}{\dot{m}_{lpc}(h_2 - h_1) + \dot{m}_{hpc}(h_4 - h_3)} \tag{2.22}$$

The equations pertaining to exergy balance of two-stage VCR system are not presented and the same can be easily reproduced with the background presented earlier in this chapter. The exergetic efficiency is given by the equation (2.23).

$$\eta_{e_x} = \frac{\dot{Q}_e \left| \left(1 - \frac{T_0}{T_r}\right) \right|}{\dot{W}_{comp_{lpc}} + \dot{W}_{comp_{hpc}}} = \text{COP}_{ts} \left| \left(1 - \frac{T_0}{T_r}\right) \right| = \frac{\text{COP}_{ts}}{\text{COP}_{rr}} \tag{2.23}$$

2.4.2.3 Results and Discussion

Figure 2.18 shows the comparison of results of Zubair *et al.* (1996), Zubair and Shaw (1986) and the theoretical model discussed in section 2.4.2.2. The values obtained from theoretical model are within ±5% of the theoretical and experimental values specified in above works. The minor difference between the theoretical and experimental results occurs due to the assumption that isentropic efficiency of compressor is invariable. In a real system, the isentropic efficiency of compressor is a function of evaporator and condenser pressures.

In order to show the enhancement of the two-stage compression cycle performance with respect to single-stage cycle, the following normalized forms of COP, irreversibility and exergetic efficiency are introduced: $\text{COP}_n = \text{COP}_{ts} / \text{COP}_{ss}$ where *n* represents normalized, *ts* two-stage and *ss* single stage. Similarly, normalized irreversibility is given by $\dot{I}_n = \dot{I}_{ts} / \dot{I}_{ss}$ and normalized exergetic efficiency by $\eta_{ex_n} = \eta_{ex_{ts}} / \eta_{ex_{ss}}$.

The data specified below for the computation of the base results is referred from Ouadha *et al.* (2005).

1. Cooling capacity (Q_e) : 3.5167 kW
2. Isentropic efficiency of compressors, (η_{comp}) : 80 %
3. Evaporator temperature, (T_e) : – 30°C
4. Condenser temperature, (T_c) : 40°C, 55 °C
5. Refrigerants : HCFC 22, ammonia and R410A

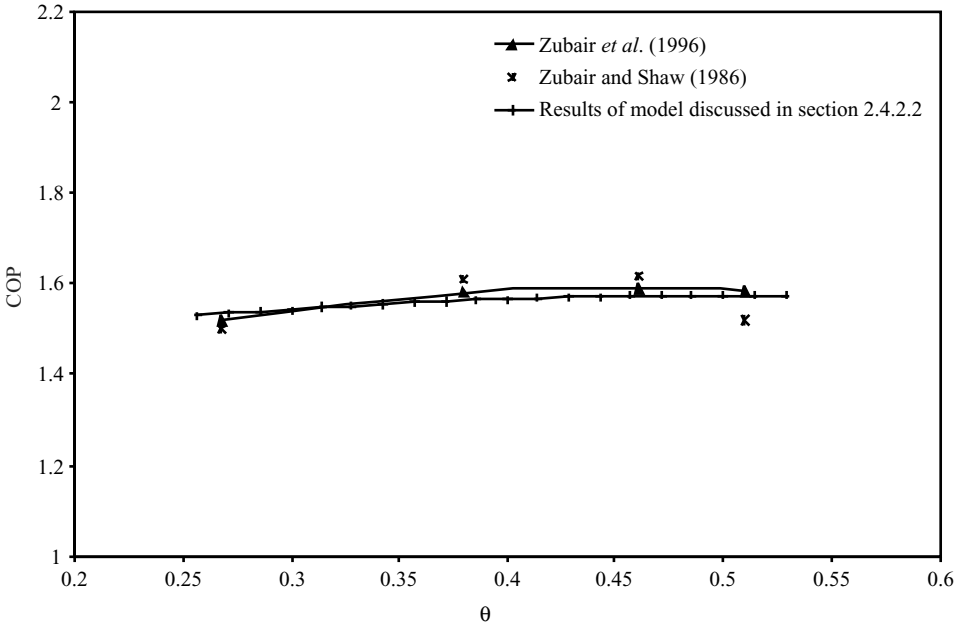

Fig. 2.18 Validation of Calculated Values (Present Work) with Calculated Values of Zubair *et al.* (1996) and Experimental Values of Zubair and Shaw (1986) (T_e = –28.89 ºC, T_c = 48.89 ºC, Refrigerant = HCFC22, Sub-cooling = 2.8ºC, Return Gas Temperature (i.e., Temperature of the Refrigerant Entering the Compressor = 18.3 ºC, η_{comp} = 65%)

Ouadha *et al.* (2005) computed the optimum inter-stage saturation temperature (pressure) for ammonia and propane. Their results were valid for two-stage system operating between a constant evaporating temperature of –30ºC and condensation temperatures of 30, 40, 50 and 60ºC. The effects of sub-cooling of refrigerant, superheating of suction vapour and variation in isentropic efficiency of compressors were not included in their study. The present study incorporates the effect of above parameters. The COP, exergetic efficiency and exergy destruction (irreversibility) are plotted as a function of the reduced inter-stage saturation temperature given by the following expression:

$$\theta = (T_i - T_e) \Big/ (T_c - T_e) \tag{2.24}$$

where T_i, T_e and T_c are intermediate, evaporation and condensation temperatures, respectively. This epresentation form is chosen to simplify the illustration of the considerable influence of the intermediate temperature (pressure) on the COP, exergy destruction (irreversibility) and exergetic efficiency of the system.

Effect of Variation in Reduced Inter-Stage Saturation Temperature (θ)

Figure 2.19 (a) and (b) are plots of normalized COP versus dimensionless reduced inter-stage saturation temperature for the refrigerants HCFC22, R410A and R717. It is observed that the normalized COP of the system first increases and then decreases with the increase in reduced inter-

stage saturation temperature. The maximum value of normailsed COP is observed to occur at an intermediate saturation temperature nearly halfway between the condensation and evaporation temperatures. The normalised COP of R410 is highest among the three refrigerants followed by HCFC22 and ammonia.

The performance of the two-stage VCR system (as compared to the single stage VCR system) increases as the difference between the condensation and evaporation temperatures increases as depicted in Fig. 2.19(b). Further, it is observed that the optimum reduced inter-stage temperature (θ_{opt}) also increases with increase in condensation temperature from 40°C to 55°C. For HCFC 22, θ_{opt} changes from 0.5143 to 0.5294, for R410A it changes from 0.5429 to 0.5647 and for R717 it increases to 0.4824 from 0.4714. The optimum inter-stage saturation temperature corresponds to the condition of minimum compressor work in both the stages. If 'θ' remains unchanged and the condenser temperature is increased, it causes the compressor work to increase in HT stage though the compressor work in LT stage remains same as previous and the total compressor work increases. As the value of 'θ' increases, it is observed that the compressor work in LT stage increases whereas in HT stage it reduces and total compressor work is also observed to reduce and it becomes minimum at 'θ_{opt}'. Moreover, the optimum inter-stage saturation temperature (θ_{opt}) is near to arithmetic mean of evaporator and condenser temperatures (Zubair and Khan, 1995; Zubair *et al.* 1996), hence it is clear that 'θ_{opt}' increases with increase in condenser temperature for a constant value of evaporator temperature.

Figure 2.20 (a) and (b) represents the effect of reduced inter-stage saturation temperature on exergetic efficiency. The trends of exergetic efficiency curves are exactly same as that of normalized COP versus reduced inter-stage saturation temperature. Another important point to note here is that maximum exergetic efficiency and maximum COP occur for identical value of θ_{opt} as shown in Fig. 2.21. This happens because both normalized COP and normalized exergetic efficiency have same formulae as proved below.

$$\mathrm{COP}_n = \frac{\mathrm{COP}_{ts}}{\mathrm{COP}_{ss}} = \frac{\dot{Q}_e / \dot{W}_{comp}}{\dot{Q}_e / (\dot{W}_{comp_{lpc}} + \dot{W}_{comp_{hpc}})} \tag{2.25}$$

$$\eta_{exn} = \frac{\eta_{ex_{ts}}}{\eta_{ex_{ss}}} = \frac{\dot{Q}_e \left|1 - T_0 / T_r\right| / \dot{W}_{comp}}{\dot{Q}_e \left|1 - T_0 / T_r\right| / (\dot{W}_{comp_{lpc}} + \dot{W}_{comp_{hpc}})} = \mathrm{COP}_n \tag{2.26}$$

Figure 2.22 is a plot showing the normalized irreversibility (exergy destruction) versus reduced inter-stage saturation temperature. This graph is an exact mirror image of the graphs of the normalized COP and normalized irreversibility versus reduced inter-stage saturation temperature. The effect of variation in condensation temperature, though not shown in this graph, can be easily predicted, i.e., with increase in condensation temperature the dimensionless irreversibility reduces since dimensionless exergetic efficiency is increasing.

Effect of Sub-cooling, Superheating and Compressor Efficiency on Optimum Inter-stage Saturation Temperature

Figure 2.23 (a), (b) and (c) shows the effect of sub-cooling, superheating and compressor efficiency on the reduced inter-stage saturation temperature for refrigerants HCFC22, R410A and R717

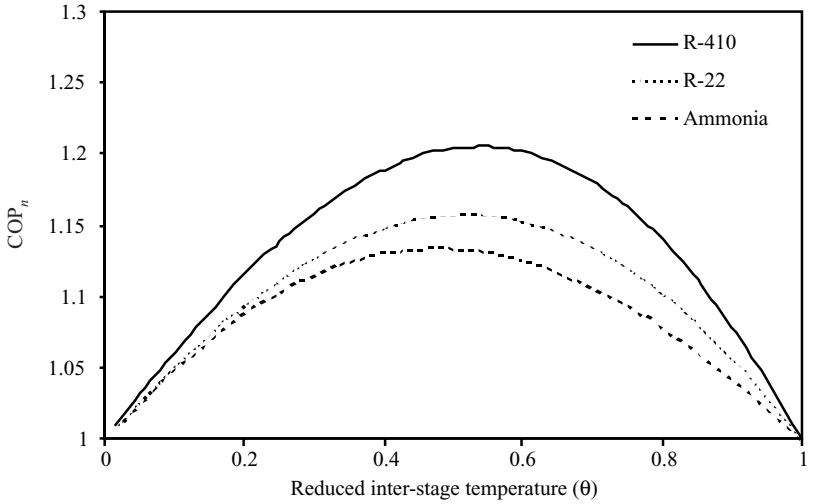

Fig. 2.19(a) Variation of Normalized COP versus Reduced Inter-stage Saturation Temperature (T_c = 40ºC)

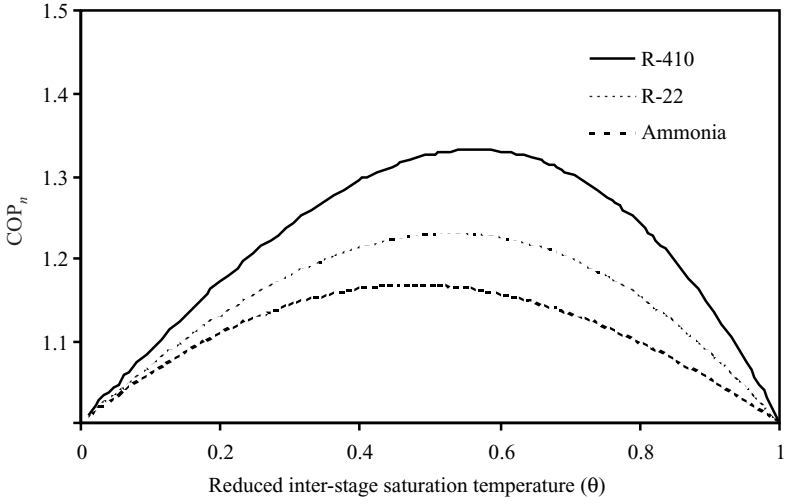

Fig. 2.19(b) Variation of Normalized COP versus Reduced Inter-stage Temperature (T_c = 55 ºC)

respectively. It is observed that optimum inter-stage saturation temperature (θ_{opt}) increases with increase in condensation temperatures for HCFC22 and R410A. Reducing the evaporation temperature does have minute influence on θ_{opt} for HCFC22 and R410A in comparison to R717. In case of R717, the θ_{opt} reduces by about 1.6%. Reducing the compressor efficiency by 10% increases the

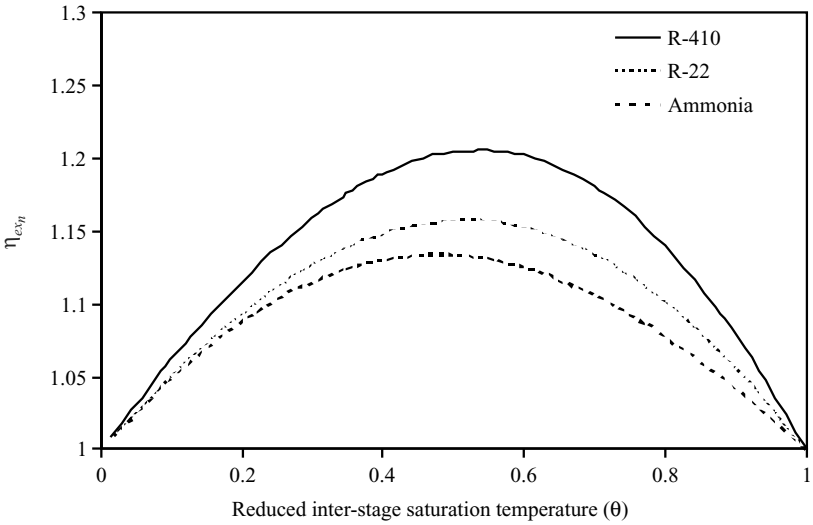

Fig. 2.20(a) Normalised η_{ex} versus Reduced Inter-stage Saturation Temperature (T_c = 40ºC)

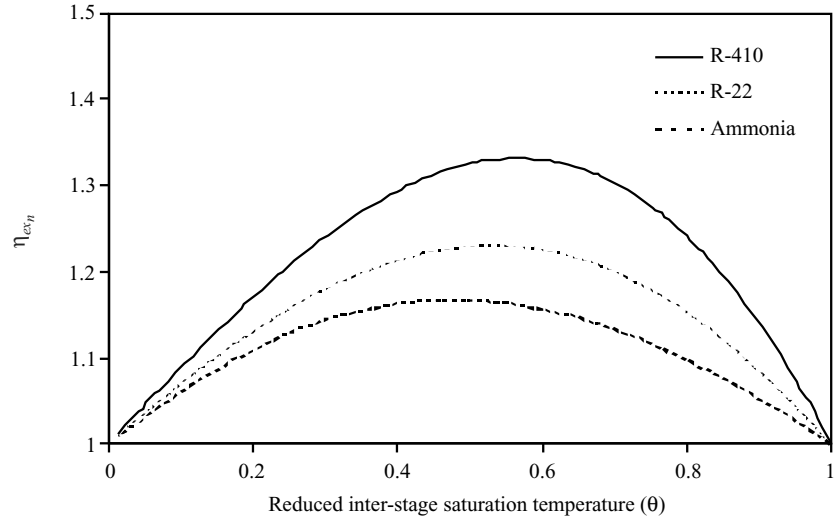

Fig. 2.20(b) Normalised η_{ex} versus Reduced Inter-stage Saturation Temperature (T_c = 55ºC)

θ_{opt} approximately by 2% for HCFC22 and R410A whereas for R717, the value of θ_{opt} increases by about 0.2 to 0.3%. Superheating the suction vapour by 10ºC brings down the θ_{opt} by about 2% for HCFC22 and R410A at lower values of condensation temperatures between 30ºC and 50ºC. However, at condensation temperatures higher than 50ºC, θ_{opt} increases in comparison to θ_{opt} when there is no superheating. This increase is however insignificant. The influence of superheating of suction vapour for R717 is significant. It is observed that θ_{opt} reduces by about 6.5% at 30ºC condensation

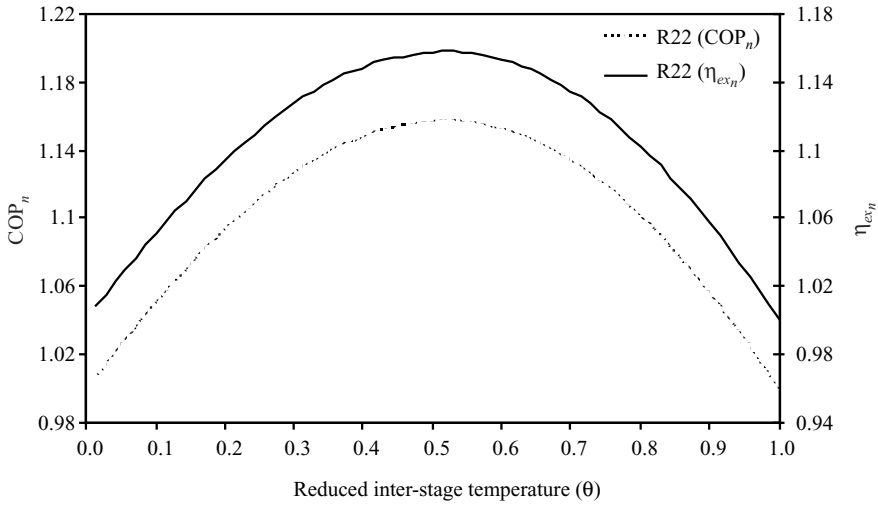

Fig. 2.21 Normalized COP and Normalized η_{ex} for HCFC22 (T_c = 40ºC)

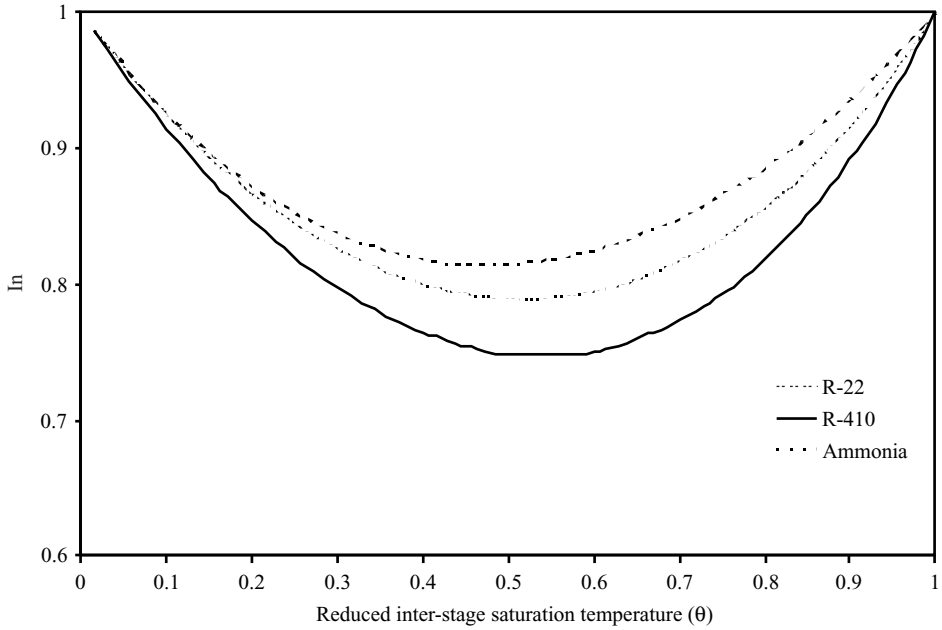

Fig. 2.22 Normalised Irreversibility versus Reduced Inter-stage Saturation Temperature (T_c = 40°C)

temperature. With increase in condensation temperature above 30ºC, the rate of decrease in θ_{opt} decreases. At 60ºC condensation temperature θ_{opt} is about 3.87% lower than the value of θ_{opt} when there was no superheating. The considerable decrease in optimum reduced inter-stage saturation temperature is observed when sub-cooling by 5ºC/10ºC is carried out (for HCFC22 and R410A)

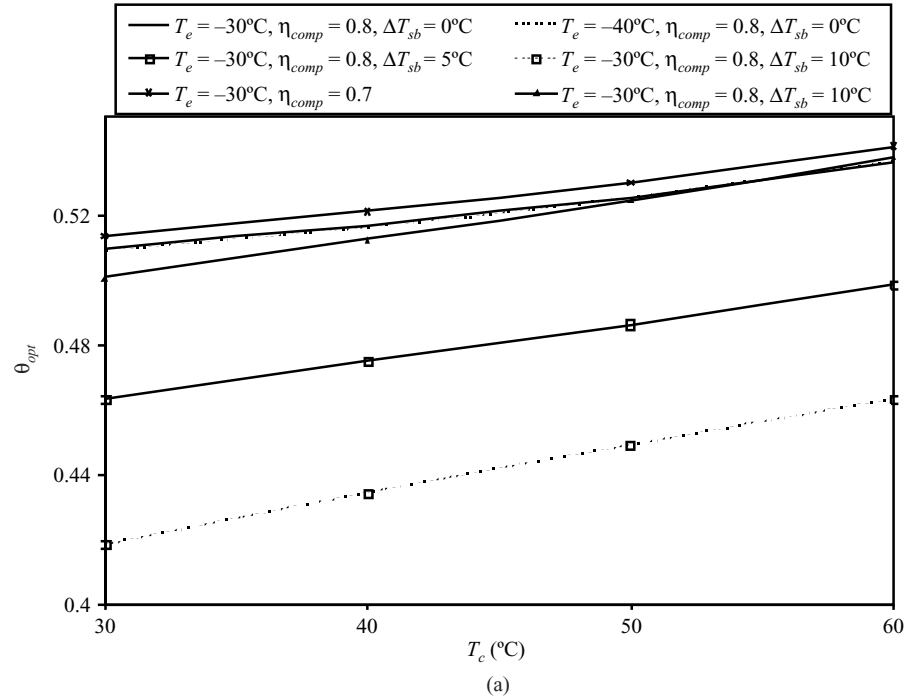

(a)

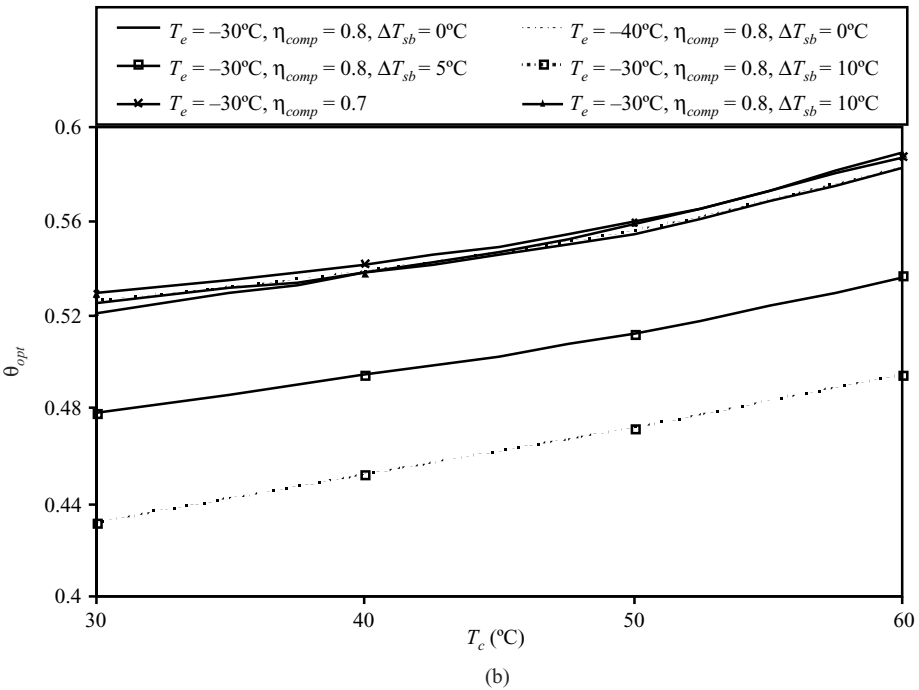

(b)

Fig. 2.23 Variation of Reduced Optimum Inter-stage Saturation Temperature versus Condenser Temperature for (a) HCFC22 (b) R410A

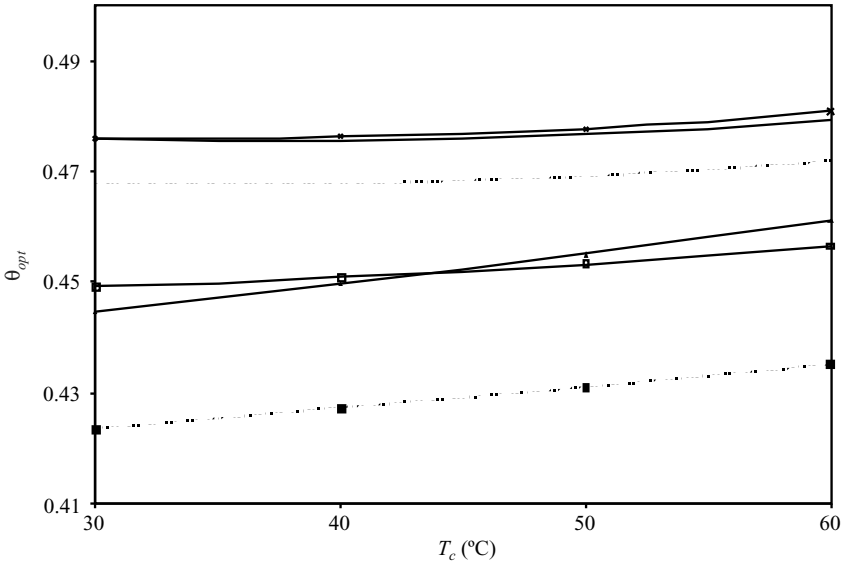

Fig. 2.23(c) Variation of Optimum Reduced Inter-stage Temperature versus Condenser Temperature for R717

which reduces the optimum inter-stage temperature by about 9%/18%. For R717, the value of θ_{opt} reduces by about 4.7%-5.7% for sub-cooling equal to 5ºC. The value of θ_{opt} reduces by about 9.2% to 11% with increase in sub-cooling, i.e., sub-cooling by 10ºC.

Tables 2.5-2.10 show the comparison of optimum inter-stage saturation temperature with AMT (arithmetic mean of evaporation and condensation temperatures) and GMT (geometric mean of evaporation and condensation temperatures), maximum COP and maximum exergetic efficiency with corresponding values of COP and exergetic efficiency for AMT and GMT respectively corresponding to various operating conditions (fixed operating conditions are: T_e = –30ºC, T_c = 30ºC, AMT = 0ºC, GMT = –1.65ºC). Table 2.5 shows the results of an ideal two-stage cycle with isentropic efficiencies of LP and HP compressors as 100%. It is observed that optimum inter-stage saturation temperature for HCFC22 and R410A is higher than AMT (0°C) and GMT (–1.65°C). The optimum inter-stage saturation temperature for R717 is lower than AMT and nearer to GMT. Table 2.6 shows the effect of reducing isentropic efficiencies of compressors from 100% to 80%. It is observed that there is minute increase in optimum inter-stage saturation temperature with decrease in isentropic efficiencies of LP and HP compressors. The corresponding values of maximum COP and maximum exergetic efficiency also reduce. The value of optimum inter-stage saturation temperatures for HCFC22 and R410A is near to AMT whereas for R717, it is near to GMT.

Tables 2.7 and 2.8 illustrate the effect of sub-cooling in condenser on the Ti_{opt}, COP_{max} and maximum exergetic efficiency. The effect of sub-cooling is to reduce Ti_{opt} and increase COP_{max} and maximum exergetic efficiency. The value of Ti_{opt} drops down below GMT due to sub-cooling. With increase in sub-cooling from 5°C to 10°C, the difference between Ti_{opt} and GMT increases. The maximum values of COP and exergetic efficiency also increase by sub-cooling.

Table 2.5 Comparison of Ti_{opt}, AMT and GMT, COP_{max}, COP_{amt} and COP_{gmt} and $\eta_{ex_{max}}$, $\eta_{ex_{amt}}$ and $\eta_{ex_{gmt}}$ for Ideal Two-stage Cycle ($\eta_{comp_{LP}} = \eta_{comp_{HP}} = 1$)

Refrigerant	Ti_{opt} (°C)	COP_{max}	$\eta_{ex_{max}}$ (%)	COP_{amt}	$\eta_{ex_{amt}}$ (%)	COP_{gmt}	$\eta_{ex_{gmt}}$ (%)
HCFC22	0.36	3.52	62.83	3.52	62.82	3.52	62.79
R410A	1.28	3.45	61.49	3.44	61.47	3.44	61.39
R717	-1.53	3.55	63.32	3.54	63.29	3.55	63.31

Table 2.6 Comparison of Ti_{opt}, AMT and GMT, COP_{max}, COP_{amt} and COP_{gmt} and $\eta_{ex_{max}}$, $\eta_{ex_{amt}}$ and $\eta_{ex_{gmt}}$ for Two-stage Cycle ($\eta_{comp_{LP}} = \eta_{comp_{HP}} = 0.8$)

Refrigerant	Ti_{opt} (°C)	COP_{max}	$\eta_{ex_{max}}$ (%)	COP_{amt}	$\eta_{ex_{amt}}$ (%)	COP_{gmt}	$\eta_{ex_{gmt}}$ (%)
HCFC22	0.60	2.77	49.49	2.77	49.48	2.77	49.46
R410A	1.53	2.71	48.42	2.71	48.40	2.71	48.35
R717	–1.52	2.8	49.89	2.79	48.87	2.79	49.88

Table 2.7 Comparison of Ti_{opt}, AMT and GMT, COP_{max}, COP_{amt} and COP_{gmt} and $\eta_{ex_{max}}$, $\eta_{ex_{amt}}$ and $\eta_{ex_{gmt}}$ for Two-stage Cycle ($\eta_{comp_{LP}} = \eta_{comp_{HP}} = 0.8$, $\Delta T_{sb} = 5$°C)

Refrigerant	Ti_{opt} (°C)	COP_{max}	$\eta_{ex_{max}}$ (%)	COP_{amt}	$\eta_{ex_{amt}}$ (%)	COP_{gmt}	$\eta_{ex_{gmt}}$ (%)
HCFC22	–2.21	2.83	50.48	2.83	50.44	2.83	50.47
R410A	–1.3	2.78	49.62	2.77	49.59	2.77	49.61
R717	–3.13	2.83	50.47	2.82	50.41	2.82	50.44

Table 2.8 Comparison of Ti_{opt}, AMT and GMT, COP_{max}, COP_{amt} and COP_{gmt} and $\eta_{ex_{max}}$, $\eta_{ex_{amt}}$ and $\eta_{ex_{gmt}}$ for Two-stage Cycle ($\eta_{comp_{LP}} = \eta_{comp_{HP}} = 0.8$ and $\Delta T_{sb} = 10$°C)

Refrigerant	Ti_{opt} (°C)	COP_{max}	$\eta_{ex_{max}}$ (%)	COP_{amt}	$\eta_{ex_{amt}}$ (%)	COP_{gmt}	$\eta_{ex_{gmt}}$ (%)
HCFC22	– 4.91	2.89	51.5	2.88	51.34	2.88	51.43
R410A	– 4.1	2.85	50.87	2.84	50.74	2.85	50.82
R717	– 4.86	2.87	51.2	2.85	50.93	2.86	51

Table 2.9 shows the effect of superheating of suction vapour on the Ti_{opt}, COP_{max} and maximum exergetic efficiency. The superheating of the suction vapour minutely reduces the Ti_{opt} for HCFC22 and R410A. For R717, Ti_{opt} reduces by 1.85°C. The maximum COP and maximum exergetic

Table 2.9 Comparison of Ti_{opt}, AMT and GMT, COP_{max}, COP_{amt} and COP_{gmt} and $\eta_{ex_{max}}$, $\eta_{ex_{amt}}$ and $\eta_{ex_{gmt}}$ for Two-stage Cycle ($(\eta_{comp_{LP}} = \eta_{comp_{HP}} = 0.8, \Delta T_{sh} = 10°C)$

Refrigerant	Ti_{opt} (°C)	COP_{max}	$\eta_{ex_{max}}$ (%)	COP_{amt}	$\eta_{ex_{amt}}$ (%)	COP_{gmt}	$\eta_{ex_{gmt}}$ (%)
HCFC22	0.043	2.75	49.09	2.75	49.09	2.75	49.07
R410A	1.25	2.69	48.02	2.69	48.01	2.69	47.96
R717	–3.37	2.76	49.18	2.75	49.12	2.75	49.15

Table 2.10 Comparison of Ti_{opt}, AMT and GMT, COP_{max}, COP_{amt} and COP_{gmt} and $\eta_{ex_{max}}$, $\eta_{ex_{amt}}$ and $\eta_{ex_{gmt}}$ for Two-stage Cycle ($(\eta_{comp_{LP}} = \eta_{comp_{HP}} = 0.8, \Delta T_{sb} = 10°C, \Delta T_{sh} = 20°C)$

Refrigerant	Ti_{opt} (°C)	COP_{max}	$\eta_{ex_{max}}$ (%)	COP_{amt}	$\eta_{ex_{amt}}$ (%)	COP_{gmt}	$\eta_{ex_{gmt}}$ (%)
HCFC22	– 6.4	2.85	50.8	2.83	50.56	2.84	50.67
R410A	–5.1	2.81	50.15	2.8	49.97	2.8	50.07
R717	–11.1	2.8	49.91	2.77	49.45	2.78	49.58

efficiency also reduce with superheating of suction vapour. The Ti_{opt} is nearer to AMT for HCFC22 and R410A whereas Ti_{opt} for R717 is nearer to GMT.

The combined effect of reducing isentropic efficiencies of LP and HP compressors, sub-cooling and superheating on Ti_{opt}, coefficients of performances and exergetic efficiencies is presented in Table 2.8. The combined effect of these parameters lowers the value of Ti_{opt} even below than that obtained in previous cases. The maximum values of COP and exergetic efficiency are higher in comparison to the maximum values of COPs and exergetic efficiencies obtained for the cases presented in Tables 2.6 and 2.9. The optimum values of inter-stage saturation temperatures for HCFC22, R410A and R717 are lower than both AMT and GMT.

Table 2.11 shows the difference between the Ti_{opt}, AMT and GMT, percentage change in values of maximum COP and exergetic efficiency with reference to values given in Table 2.6. It is observed that the optimum value of inter-stage temperatures for HCFC22 and R410A are nearer to AMT when isentropic efficiencies of compressors are assumed to be lower than 100% and superheating is considered in evaporator.

The optimum value of inter-stage saturation temperature for HCFC22 and R410A is nearer to GMT when either sub-cooling is considered or in the case of cycle with sub-cooling, superheating and isentropic efficiencies of compressors are less than 100%. The optimum value of inter-stage temperature for R717 is closer to GMT under all conditions considered in this analysis.

Table 2.12 illustrates the comparison of optimum inter-stage temperature, AMT and GMT for the following conditions: T_e = –30°C, $\eta_{comp_{LP}} = \eta_{comp_{HP}} = 0.8$, ΔT_{sb} = 10°C, ΔT_{sh} = 20°C for condensation temperatures 40, 50 and 60°C. It is observed that optimum inter-stage saturation

Table 2.11 Difference Between the Ti_{opt}, AMT and GMT, Percentage Change in Values of Maximum COP and Exergetic Efficiency with Reference to Values Given in Table 2.6.

Table No. '*i*'	Refrigerant	Difference between *AMT* and Ti_{opt}	Difference between *GMT* and Ti_{opt}	Percentage change in the value of COP_{max} (value corresponding to table no. '*i*') with reference to the value given in Table 2.6	Percentage change in the value of $\eta_{ex_{max}}$ (value corresponding to table no. '*i*') with reference to the value given in Table 2.6
2.6	HCFC22	***0.6***	2.25	------	------
2.7	HCFC22	–2.21	**–0.56**	1.98	1.98
2.8	HCFC22	– 4.91	**–3.26**	4.22	4.06
2.9	HCFC22	***0.043***	1.69	– 0.81	– 0.81
2.10	HCFC22	– 6.4	**– 4.74**	2.67	2.65
2.6	R410A	***1.53***	3.18	------	------
2.7	R410A	–1.3	**0.35**	2.45	2.45
2.8	R410A	– 4.1	**–2.44**	5.04	5.05
2.9	R410A	***1.25***	2.9	– 0.83	– 0.83
2.10	R410A	–5.1	**–3.42**	3.57	3.57
2.6	R717	–1.52	**0.13**	------	------
2.7	R717	–3.13	**–1.48**	1.17	1.18
2.8	R717	– 4.86	**–3.21**	2.61	2.62
2.9	R717	–3.37	**–1.72**	– 1.4	– 1.41
2.10	R717	–11.1	**– 9.46**	0.064	0.054

The values in **bold** show the proximity of optimum inter-stage temperature to GMT and values in ***italic bold*** show the proximity of optimum inter-stage temperature to AMT.

temperature is nearer to GMT except for the case of R410 at 60ºC condensation temperature. In this case the optimum temperature is nearer to AMT.

Table 2.12 Comparison of Optimum Inter-stage Temperature, AMT and GMT at Various Condensation Temperatures ($T_e = -30$°C, $\eta_{comp_{LP}} = \eta_{comp_{HP}} = 0.8$, $\Delta T_{sb} = 10$°C, $\Delta T_{sh} = 20$°C)

Refrigerant	Condensation Temperature (T_c in °C)								
	40			50			60		
	Ti_{opt} (°C)	AMT (°C)	GMT (°C)	Ti_{opt} (°C)	AMT (°C)	GMT (°C)	Ti_{opt} (°C)	AMT (°C)	GMT (°C)
HCFC22	– 0.62	5	2.79	5.37	10	7.16	11.6	15	11.46
R410A	1.2	5	2.79	7.86	10	7.16	15.18	15	11.46
R717	– 4.25	5	2.79	0.67	10	7.16	12.19	15	11.46

Thus, it can be concluded that optimum inter-stage saturation pressure of an actual two-stage refrigeration system is closer to saturation pressure corresponding to GMT of condensation and evaporation temperatures.

Thus two-stage VCR system is examined with a viewpoint to obtain optimum inter-stage saturation temperature for HCFC22, R410A and R717 and further the effects of various parameters have also been investigated on the optimum inter-stage saturation temperature.

2.4.3 Cascade Refrigeration System

Bansal and Jain (2007) reviewed the literature on cascade refrigeration system. They reported that a cascade refrigeration system is normally required for producing low temperatures ranging from (–)30°C to (–)100°C for various industries such as pharmaceutical, food, chemical, blast freezing and liquefaction of gases. The refrigerants specified for use in high temperature circuit are HCFC22, HFC134a, R507A, ammonia, propane, and propylene whereas carbon dioxide, HFC23 and R508B are suitable for use in low temperature circuit. The refrigerant pairs that have received the most attention in recent years are R717/R744 (ammonia/carbon-dioxide) and R1270/R744 (propylene / carbon dioxide) for applications down to (–) 54°C.

Kanoglu (2002) accomplished the exergy analysis of the multistage cascade refrigeration cycle used for natural gas liquefaction. The relations for the total exergy destruction, exergetic efficiency and minimum work requirement for the liquefaction of natural gas in the cycle were developed. It was shown that the minimum work depends only on the properties of the incoming and outgoing streams of natural gas.

Agnew and Ameli (2004) optimized two-stage cascade refrigeration system using finite time thermodynamics approach for refrigerant R717 and R508b in high temperature and low temperature circuits respectively. This pair was found to exhibit better performance in comparison to R12 and R13 pair.

Nicola *et al*. (2005) carried out the first law performance of a cascade refrigeration cycle, operating with ammonia in high temperature circuit and blends of CO_2 and HFCs in low temperature circuit, for those applications where temperatures below triple point of CO_2 (216.58 K) are needed. Their results revealed that the R744 blends are an attractive option for the low-temperature circuit of cascade systems operating at temperatures approaching 200 K.

Bhattacharyya *et al*. (2005) carried out the analysis of a cascade refrigeration system for simultaneous heating and cooling with a CO_2 based high temperature cycle and C_3H_8 (propane)

based low temperature cycle. They predicted the optimum performance of the system with variation in the design parameters and operating variables. This cascaded system can operate simultaneously between refrigerating space temperature of –40°C and a heating output temperature of about 120°C. Moreover, propane vindicates itself as a better refrigerant than ammonia due to its non-toxic nature. However, its flammability remains a concern.

Lee *et al.* (2006) optimised condensing temperature of a two-stage cascade refrigeration system for ammonia and carbon dioxide for maximization of COP and minimization of exergy loss. It was deduced that optimal condensing temperature increased with condensation and evaporation temperatures. The effects of sub-cooling and superheating were not taken into consideration. The computation of exergetic efficiency was also not performed.

Kruse and Rüssmann (2006) investigated the COP of a cascade refrigeration system using N_2O (nitrous oxide) as refrigerant for the low temperature cascade stage and various natural refrigerants like NH_3 (ammonia), C_3H_8, propene, CO_2 and N_2O itself for the high temperature stage. They compared its result with a conventional CFC23/HFC134a cascade refrigeration system for heat rejection temperatures between 25 and 55°C. They concluded that by substituting the lower stage refrigerant CFC23 by N_2O practically achieved the same energetic performance with high stage fluids HFC134a, ammonia and hydrocarbons.

Niu and Zhang (2007) carried out the experimental study of a cascade refrigeration system with R290 in high temperature circuit and a blend of R744/R290 in low temperature circuit. The performance of the blend was compared with R13 in low temperature circuit. The blend showed good cycle performance compared with R13 and is considered a promising alternative refrigerant to R13 when the evaporator temperature is higher than 201 K.

Getu and Bansal (2008) carried out energy analysis of a carbon dioxide-ammonia (R744-R717) cascade refrigeration system. Their study involved the examination of the effects of evaporating, condensing and cascade condenser temperatures, sub-cooling and superheating in both high and low temperature circuits on optimum COP. They employed a multi-linear regression analysis and developed mathematical expressions for maximum COP, the optimum evaporating temperature of R717 and the optimum mass flow ratio of R717 to that of R744 in the cascade system. Their study did not include the exergy analysis approach to achieve maximum exergetic efficiency.

Dopazo *et al.* (2009) carried out theoretical analysis of a CO_2-NH_3 cascade refrigeration system for cooling applications at low temperatures. The results have been presented for optimization of coefficient of performance in the evaporation temperature range (–)55°C to (–)30°C in low temperature circuit, 25 to 50°C condensation temperature in high temperature circuit and (–)25 to 5°C in cascade condenser. The approach temperature was varied between 3 and 6°C. The effect of compressor isentropic efficiency on system COP is also examined. The results show that, when following both exergy analysis and energy optimization methods, an optimum value of cascade condenser temperature is achieved. However, in this study, effect of sub-cooling and superheating for determining the optimum cascade condenser temperatures is not included.

2.4.3.1 Description of Cascade Vapour Compression Refrigeration System

A cascade refrigeration system is used for applications in temperature range between (–)30°C and (–)100°C for cold storage and liquefaction of gases, etc.

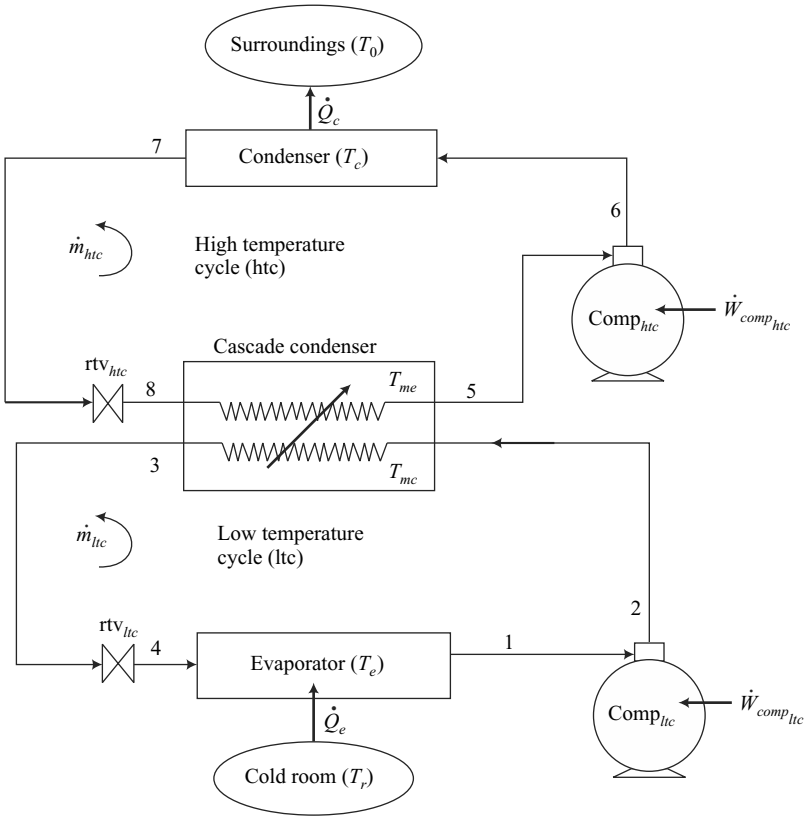

Fig. 2.24(a) Schematic Diagram of a Cascade Refrigeration System

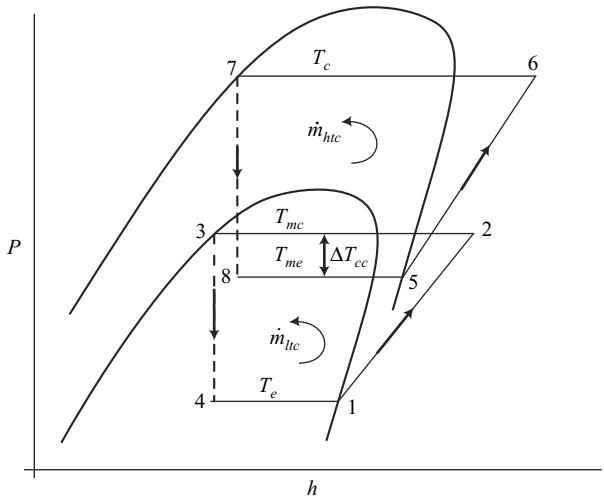

Fig. 2.24(b) P-h Diagram of Cascade Refrigeration System

Figure 2.24(a) schematically represents a two-stage cascade VCR system and Fig. 2.24(b) represents the corresponding pressure enthalpy diagram. This refrigeration system comprises two separate refrigeration cycles—the high-temperature cycle (htc) and the low-temperature cycle (ltc). Each cycle has a different refrigerant suitable for that temperature with lower temperature units progressively using lower boiling point refrigerants.

The lower boiling point refrigerant will have higher saturation pressure at low temperatures that keeps the ingress of air under control and requires a smaller compressor for the same refrigerating effect due to higher density of suction vapours. The cycles are thermally connected to each other through a cascade-condenser, which acts as an evaporator for the 'htc' and a condenser for the 'ltc'. Figure 2.24(a) indicates that the condenser in this cascade refrigeration system rejects heat Q_c from the condenser at condensing temperature T_c to its warm coolant or environment at temperature T_0. The evaporator of the cascade system absorbs refrigeration load $\dot{Q}_e$ from the cold refrigerated space at T_r to the evaporating temperature T_e. The heat absorbed by the evaporator of the ltc plus the work input to the ltc compressor equals the heat absorbed by the evaporator of the htc. T_{mc} and T_{me} represent the condensing and evaporating temperatures of the cascade condenser, respectively. Approach is designated as ΔT_{cc} and it represents the difference between the condensing temperature (T_{mc}) of ltc and the evaporating temperature (T_{me}) of htc. The evaporating temperature (T_e), the condensing temperature (T_c), and the temperature difference in the cascade-condenser (ΔT_{cc}) are three important design parameters of a cascade refrigeration system.

Thermodynamic Analysis of Cascade Refrigeration System

The thermodynamic analysis of the two-stage cascade refrigeration system involves the application of principles of mass conservation, energy conservation and exergy balance as discussed earlier.

The following input data is used (Bansal and Jain (2007)) for computation of results shown in Figs. (2.19) to (2.26).

1. Refrigeration capacity (Q_e) : 1 TR
2. Sub-cooling of refrigerant leaving 'htc' condenser (ΔT_{sb}) : 5°C
3. Superheating of suction vapour in 'ltc' evaporator (ΔT_{sh}) : 10°C
4. Isentropic efficiency of compressors (η_{comp}) : 70%
5. Difference between evaporator and space temperature : ($T_r - T_e$) = 10°C
6. Evaporator temperature (T_e) (in steps of 5°C) : – 55°C to – 15°C
7. Condenser temperature (T_c) (in steps of 10°C) : 30°C to 60°C
8. Dead state temperature (T_0) and pressure (P_0) : 25°C, 1.01325 bar
9. Reference enthalpy (h_o) and entropy (s_o) of the working fluids have been calculated corresponding to the dead-state temperature (T_0) of 25°C.
10. Heat losses and pressure drops in connecting lines and various components are neglected.

Figure 2.25 (a) and (b) represent the comparison of results obtained using the computer code developed for performance analysis of two-stage cascade VCR system with research of Bansal and Jain (2007). In Fig. 2.25 (a) the variation of COP versus approach in cascade condenser is shown and in Fig. 2.25 (b) variation of COP versus temperature in cascade condenser (T_{cc}) is presented. It

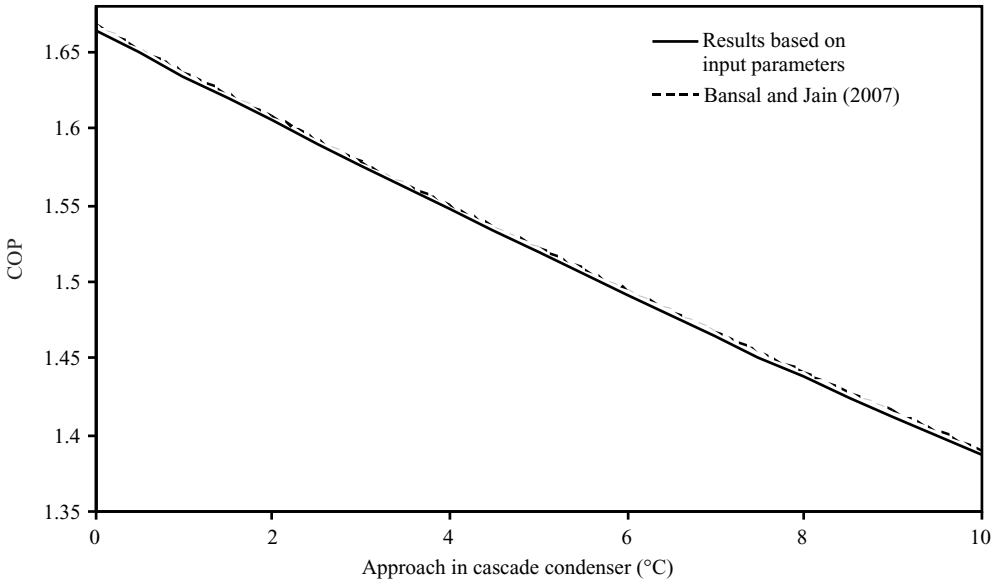

Fig. 2.25(a) Approach versus COP (Comparison of Present Work with Bansal and Jain, 2007) (R-717 in 'htc' and R-744 in 'ltc') ($T_e = -45°C$, $T_c = 30°C$, $T_{cc} = -15°C$)

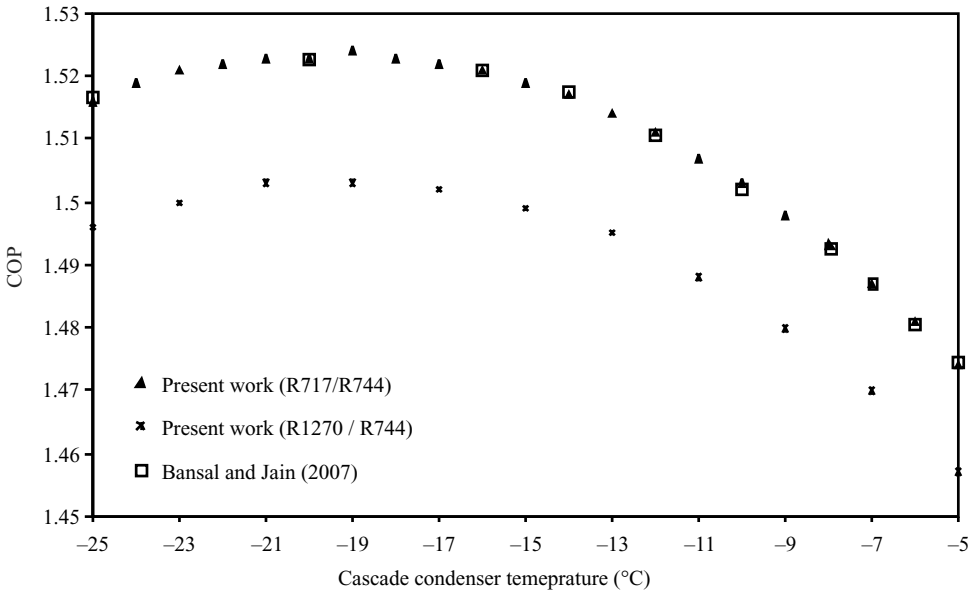

Fig. 2.25(b) Variation of COP versus T_{cc}
($T_e = -45°C$, $T_c = 30°C$, $\Delta T_{sb} = 5°C$, $\Delta T_{sh} = 10°C$, $\eta_{comp} = 0.7$, $\Delta T_{cc} = 5°C$)

is observed that results calculated using the present model are in agreement with the theoretical results reported by Bansal and Jain (2007) for ammonia/carbon dioxide pair and the difference in results is less than 0.5%. The increase in approach causes a drop in COP because of increase in cascade condenser temperature and hence pressure ratio across compressor in 'ltc' increases thereby increasing the compression work in 'ltc'. This enhancement of compression work causes a reduction in COP in 'ltc' and COP of the cascade system also. The variation of COP with temperature in cascade condenser shows that there exists a maximum value of COP corresponding to which cascade condenser temperature is optimum. This happens because the pressure ratio of 'ltc' compressor increases with increase in cascade condenser temperature causing a reduction in COP in 'ltc' because of increase in compressor work in 'ltc' whereas the reverse happens in '*htc*' and hence there exists an optimum cascade condenser temperature T_{cc-opt} corresponding to which total compression work is minimum and hence COP is maximum. The results of propylene/carbon-dioxide are also shown in this figure and it can be observed that the COP curve is identical for this pair of refrigerants however the COP offered is lower in comparison to ammonia/carbon-dioxide pair.

Effect of Cascade Condenser Temperature

Figure 2.26 presents the variation of exergetic efficiency and total exergy destruction versus cascade condenser temperature. It is observed that total exergy destruction decreases up to certain cascade condenser temperature and further increases with increase in cascade condenser temperature. The exergetic efficiency shows a reverse trend in comparison to total exergy destruction. The reason for such a behaviour of exergetic efficiency can be explained on the basis of total compressor power required in 'ltc' and 'htc'. The total compressor power required is lowest at a particular

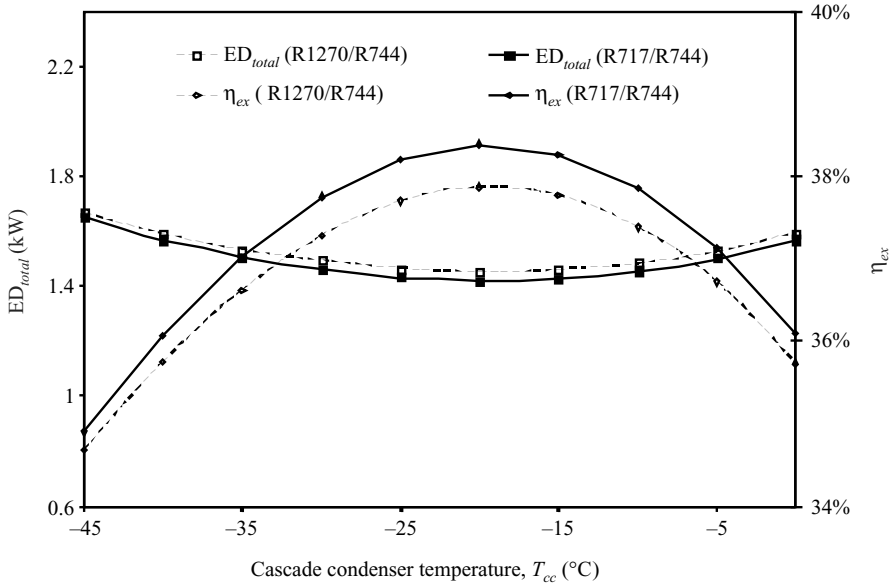

Fig. 2.26 Effect of Cascade Condenser Temperature (T_{cc}) on Total Exergy Destruction and Exergetic Efficiency (T_e = – 45°C, T_c = 30°C, ΔT_{sb} = 5°C, ΔT_{sh} = 10°C , η_{comp} = 0.7, ΔT_{cc} = 5°C)

cascade condenser temperature. The refrigeration capacity ($\dot{Q}_e$) is constant and the term $\left(1-\frac{T_0}{T_r}\right)$ is also constant since both dead state temperature (T_0) and cold room temperature (T_r) are constants. Hence, the value of input exergy expressed by $\dot{Q}_e\left(1-\frac{T_0}{T_r}\right)$ is constant. Thus, exergetic efficiency given by $\eta_{e_x}\frac{\left|\dot{Q}_e\left(1-\frac{T_0}{T_r}\right)\right|}{\dot{W}_{comp_{total}}}$ is highest at a specific cascade condenser temperature corresponding to which total compressor power required is lowest. This specific temperature, corresponding to which the exergetic efficiency is highest, is optimum cascade condenser temperature. It is observed from Figs. 2.25(b) and 2.26 that the optimum cascade condenser temperature corresponding to maximum COP and maximum exergetic efficiency is identical. Fig. 2.26 also depicts that R717/ R744 shows better exergetic efficiency as compared to R1270/R744.

The influence of various design parameters which affect the optimum cascade condenser temperature, maximum COP and maximum exergetic efficiency are (i) evaporator temperature; (ii) condenser temperature; (iii) approach in cascade condenser; (iv) isentropic efficiencies of compressors in 'ltc' and 'htc'; (v) sub-cooling of refrigerant leaving condenser in 'htc' and (vi) superheating in evaporator in 'ltc'.

Effect of Evaporator Temperature

Figure 2.27 shows the variation of optimum cascade condenser temperature and maximum COP with evaporator temperature and the influence of isentropic efficiency of 'ltc' and 'htc' compressors on optimum temperature in cascade condenser and maximum COP.

It is evident from Fig. 2.27 that the increase in evaporator temperature increases the optimum temperature in cascade condenser and maximum COP. The increase in optimum cascade condenser temperature is attributed to decrease in overall working temperature range and it also reduces the pressure ratio in 'ltc' and 'htc'. Hence, compressor work decreases and COP of the cascade system increases. It is observed that decrease in isentropic efficiency of the 'ltc' compressor from 1 to 0.8 (keeping the isentropic efficiency of compressor in 'htc' = 1) causes the optimum cascade condenser temperature to decrease whereas the reverse happens in case when isentropic efficiency of the 'htc' compressor decreases to 0.8 from 1(keeping the isentropic efficiency of the 'ltc' compressor =1). This effect is nearly compensated when the efficiencies of both 'ltc' and 'htc' compressors reduce from 1 to 0.8 and the optimum cascade condenser temperature obtained in this particular case is very near (but lower) to the optimum cascade condenser when isentropic efficiencies of both the compressors were assumed to be 1. One more observation that is important to highlight here is that 20% reduction in the efficiency of 'ltc' compressor causes about 10 K drop in optimum cascade condenser temperature as compared to about 8 K rise in cascade condenser temperature for the same decrease in efficiency of 'htc' compressor. On the other hand 20% drop in isentropic efficiency of 'ltc' compressor causes the system COP to drop by 7.3% to 8.9% as compared to a drop of 13-14% in COP for 20% decrease in isentropic efficiency of 'htc' compressor.

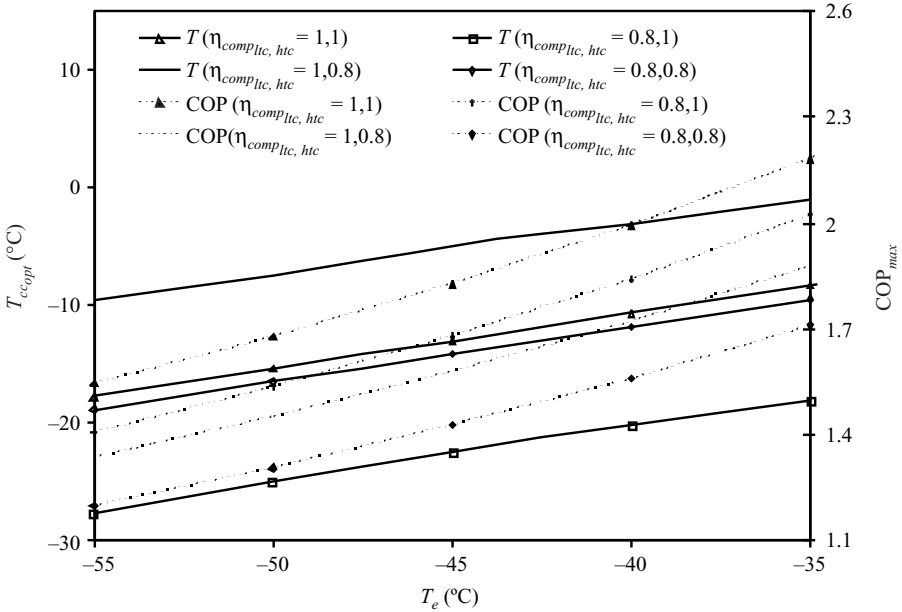

Fig. 2.27 Evaporator Temperature versus Optimum Temperature in Cascade Condenser and COP_{max} for R717/ R744 ($\Delta T_{cc} = 0$, $T_c = 50$ºC)

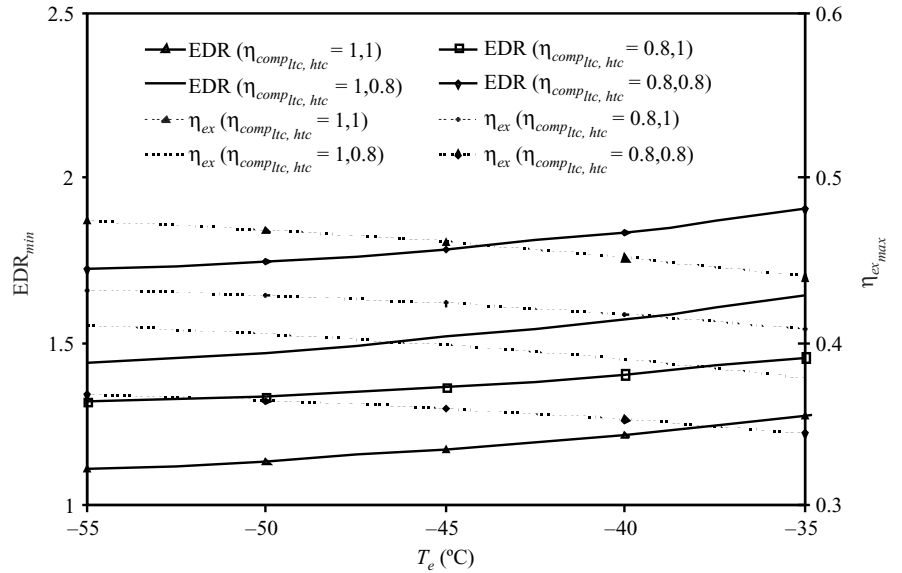

Fig. 2.28 Evaporator Temperature versus Maximum Exergetic Efficiency and Minimum EDR for R717/ R744 ($\Delta T_{cc} = 0$, $T_c = 50$ºC)

The variation in EDR_{min} and maximum exergetic efficiency is represented in Fig. 2.28. Two main characteristics of this Figure are decreasing trend of maximum exergetic efficiency with increase in evaporator temperature and decrease in maximum value of exergetic efficiency with decrease in isentropic efficiency of either of the compressors. In this case also, it is crucial to

emphasize that the reduction in isentropic efficiency of 'htc' compressor by 20% causes about 13-14% reduction in maximum value of exergetic efficiency as compared to 7.3-9% reduction when the isentropic efficiency of 'ltc' compressor reduces by same amount. Thus once again it is confirmed that lowering of isentropic efficiency of compressor in 'htc' (i.e., compressor for ammonia) has more damaging effect on system performance as compared to carbon dioxide compressor in 'ltc'. The trends of curves of minimum EDR are just opposite to maximum exergetic efficiency curves.

Figure 2.29 illustrates the effect of variation in evaporator temperature on optimum temperature in cascade condenser and maximum COP for R1270/R744 pair.

Figure 2.30 shows the effect of variation in evaporator temperature on minimum EDR and maximum exergetic efficiency. The trends for optimum cascade condenser temperature, maximum COP, maximum exergetic efficiency and minimum EDR are similar to the trends of these parameters presented in Figs. 2.27 and 2.28 for R717/R744. The 20% reduction in isentropic efficiency of 'ltc' compressor (i.e., carbon dioxide compressor) is accountable for lowering both maximum COP and maximum exergetic efficiency by 8.7% and 10.2% corresponding to evaporator temperatures of –35°C and –55°C respectively. Similar to above, the reduction in maximum values of COP and exergetic efficiency is 13.1% and 12.6% for identical temperature conditions when isentropic efficiency of 'htc' compressor reduces by 20%.

Table 2.13 presents the comparison of the two pairs of refrigerants considered for various conditions of isentropic efficiencies of 'ltc' and 'htc' compressors. It is observed that R717/R744 refrigerant pair offers better performance in terms of maximum COP and maximum exergetic efficiency as specified in the table. The values given in braces show the percentage difference by which the values of maximum COP and maximum exergetic efficiency for refrigerant pair R1270/R744 are lower than the corresponding values for R717/R744.

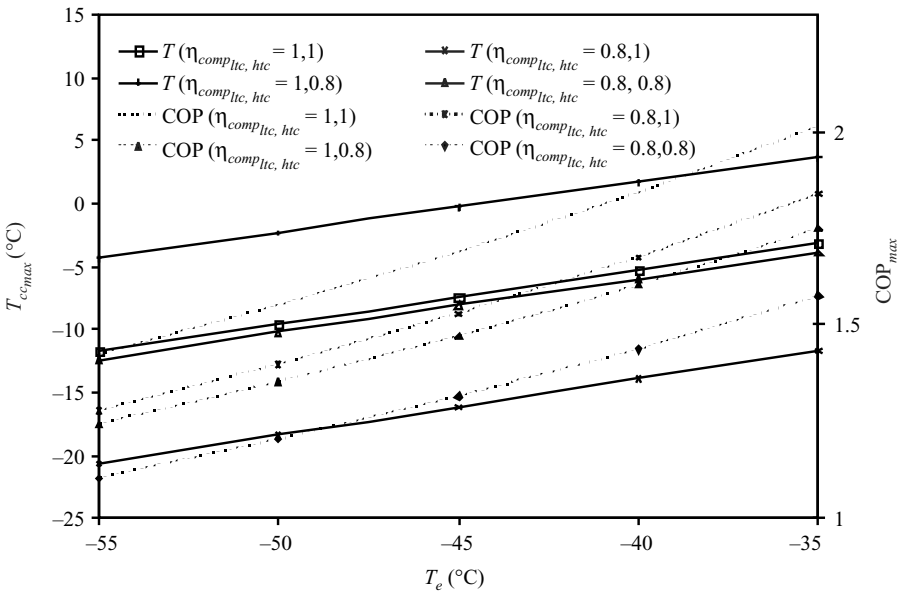

Fig. 2.29 Evaporator Temperature versus Optimum Temperature in Cascade Condenser and Maximum COP for R1270/R744 ($\Delta T_{cc} = 0$, $T_c = 50°C$)

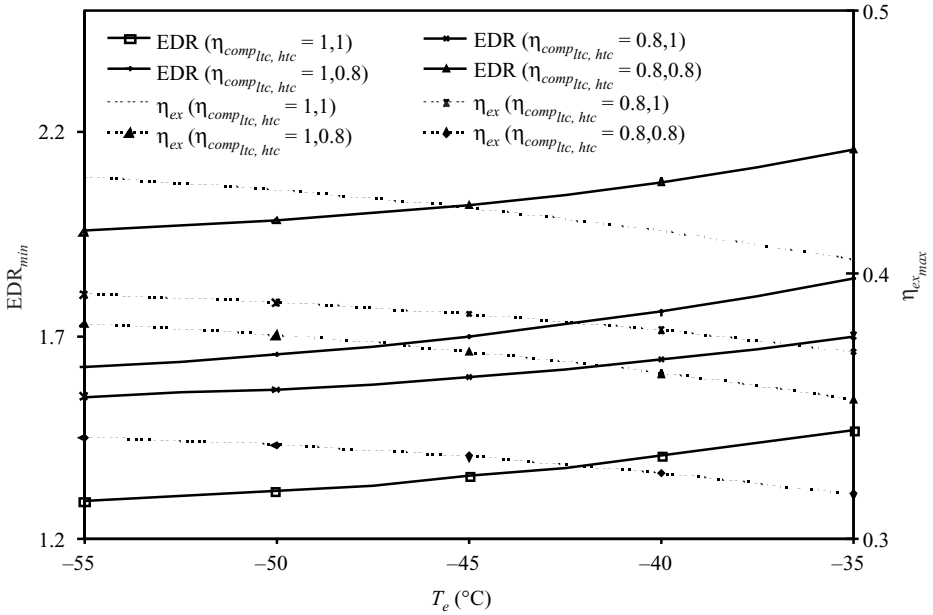

Fig. 2.30 Evaporator Temperature versus Maximum Exergetic Efficiency and Minimum EDR for R1270/R744 (ΔT_{cc} = 0, T_c = 50°C)

Table 2.13 Comparison of Optimum Cascade Condenser Temperature, COP_{max} and Maximum Exergetic Efficiency of R717/744 and R1270/R744 Pairs

ΔT_{cc} = 0°C, T_c = 50°C, T_e = – 45°C							
η_{comp}		**T_{cc} (°C)**		**COP_{max}**		**$\eta_{ex_{max}}$**	
ltc	***htc***	**R717/R744**	**R1270/R744**	**R717/R744**	**R1270/R744**	**R717/R744**	**R1270/R744**
1	1	–13.02	–7.43	1.83	1.69 (– 7.6%)	0.461	0.425 (–7.8%)
0.8	1	–22.39	–16.18	1.68	1.53 (– 8.9%)	0.423	0.385 (– 8.98%)
1	0.8	– 4.95	– 0.32	1.58	1.47 (–6.9%)	0.398	0.371 (–6.8%)
0.8	0.8	–14.16	–8.11	1.43	1.31 (–8.4%)	0.359	0.331 (–7.8%)
0.7	0.7	–15.10	– 8.66	1.23	1.13 (– 8.13%)	0.31	0.284 (–8.39%)

Effect of Condenser Temperature

Figures 2.31 and 2.32 depict the effect of condenser temperature on optimum cascade condenser temperature, maximum COP, minimum EDR and maximum exergetic efficiency respectively for

R717/R744. Simultaneously, these figures also present the effect of isentropic efficiencies 'ltc' and 'htc' compressors on the above-mentioned parameters. The optimum temperature increases with increase in condenser temperature. This happens because of increase in overall working temperature range. The maximum COP of the system reduces since the increase in condenser temperature

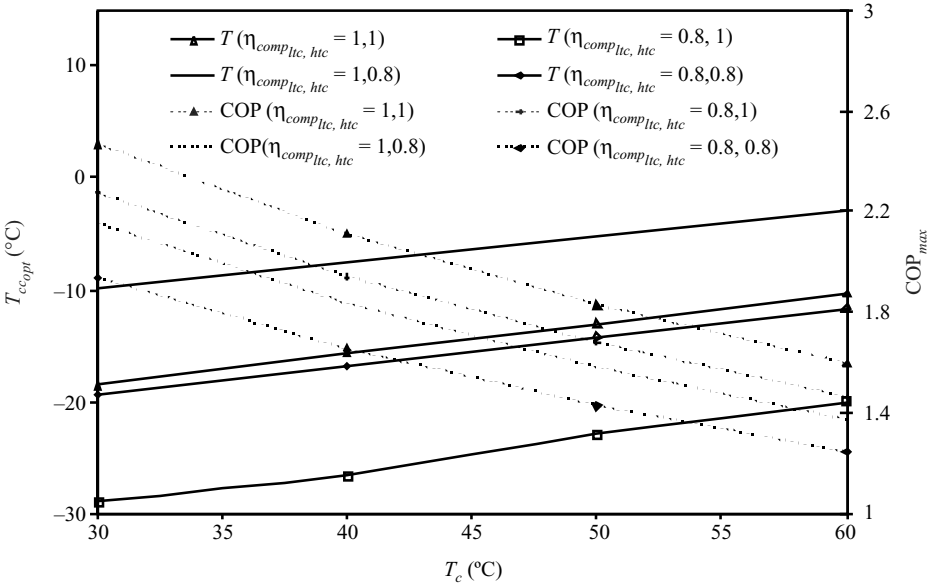

Fig. 2.31 Variation of Optimum Temperature in Cascade Condenser and Maximum COP versus Condenser Temperature for R717/ R744 ($\Delta T_{cc} = 0$, $T_e = -45$ºC)

causes the pressure ratios of the 'ltc' and 'htc' compressors to increase and hence the power input increases thereby reducing the maximum COP. The effect of isentropic efficiencies of compressors on optimum temperature in cascade condenser and maximum COP are similar to the trends observed in the case of variation of evaporator temperature depicted in Fig. 2.27 and explained in corresponding para.

Figure 2.32 shows that maximum exergetic efficiency reduces with increase in condenser temperature. This decreasing trend of exergetic efficiency is achieved because of increase in input exergy, i.e., total compressor power required for the same output exergy corresponding to a constant cooling capacity. The effect of isentropic efficiencies of the compressors is similar to the trends that were achieved in case when evaporator temperature was varied (Refer Fig. 2.28 and corresponding para).

The variation of optimum temperature in cascade condenser and maximum COP for R1270/ R744 is illustrated in Fig. 2.33. The variation in maximum exergetic efficiency and minimum *EDR* are presented in Fig. 2.34. The explanation of trends of these curves for R1270/R744 is similar to as already has been discussed for R717/R744. The comparison of the optimum temperatures, maximum COP and maximum exergetic efficiencies for a particular set of data is already presented for these two pairs of refrigerants in Table 2.13.

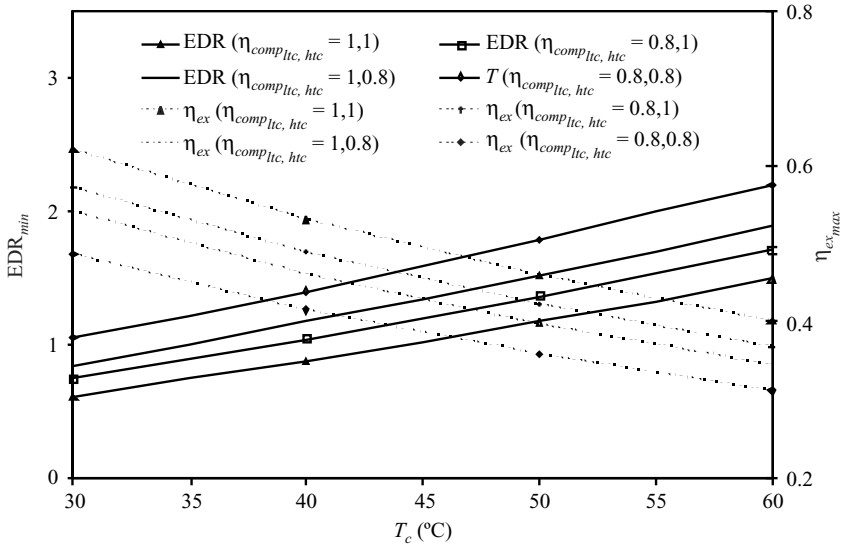

Fig. 2.32 Variation of Maximum Exergetic Efficiency and Minimum EDR versus Condenser Temperature for R717/ R744 ($\Delta T_{cc} = 0$, $T_e = -45$ºC, $T_r = T_e + 10$ ºC)

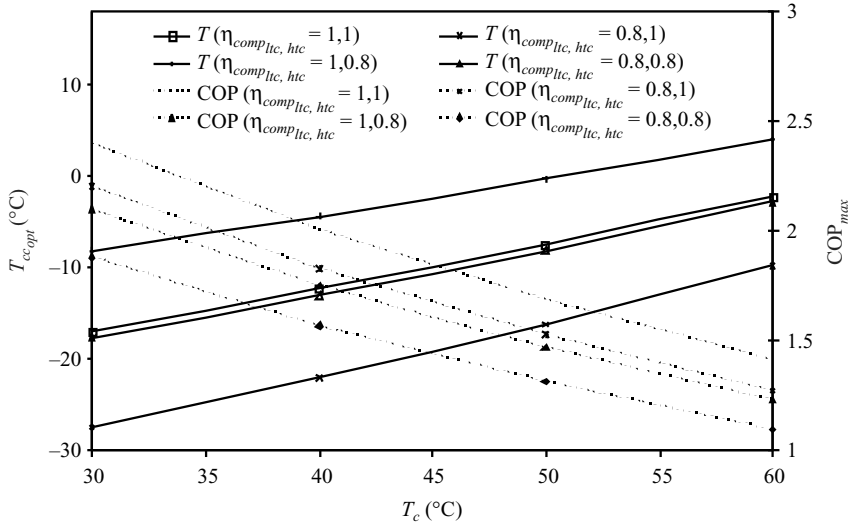

Fig. 2.33 Variation of Optimum Temperature in Cascade Condenser and Maximum COP versus Condenser Temperature for R1270/R744 ($\Delta T_{cc} = 0$, $T_e = -45$°C, $T_r = T_e + 10$°C)

Effect of Approach (ΔT_{cc})

Figures 2.35 and 2.36 represent the effect of approach on optimum temperature in cascade condenser, maximum COP and maximum exergetic efficiency for R717/R744 and R1270/R744. It is observed that the increase in approach causes increase in optimum temperature in cascade condenser. Further

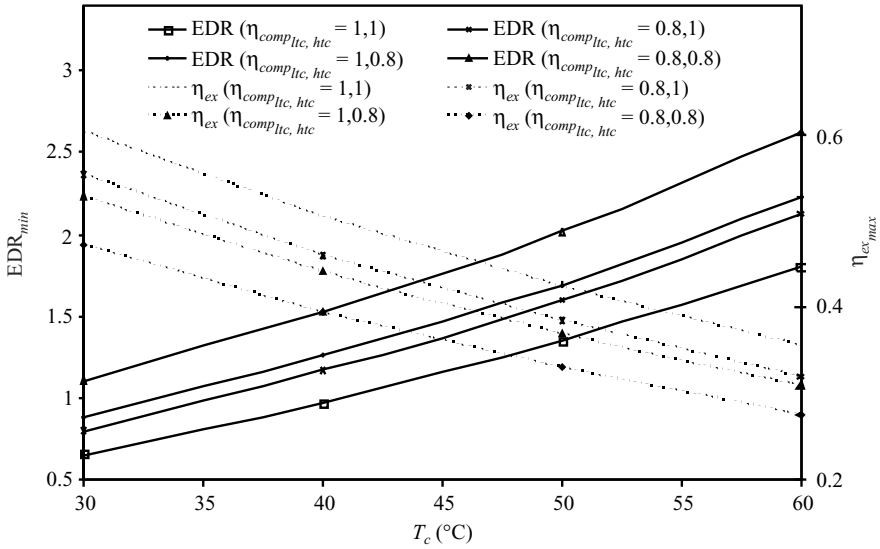

Fig. 2.34 Condenser Temperature versus Maximum Exergetic Efficiency and Minimum EDR for R1270/R744 ($\Delta T_{cc} = 0$, $T_e = -45$°C, $T_r = T_e + 10$°C)

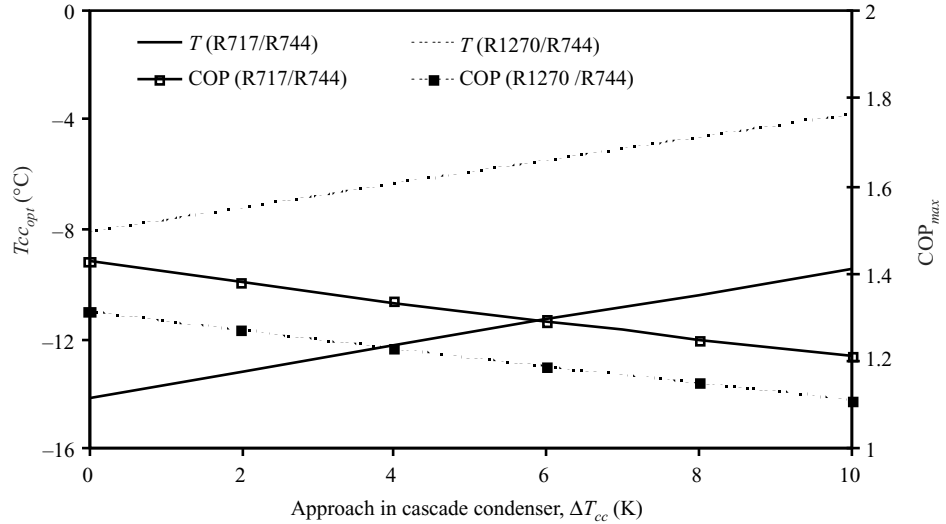

Fig. 2.35 Variation of Optimum Temperature in Cascade Condenser and Maximum COP with Approach (ΔT_{cc}) in Cascade Condenser for R717/R744 and R1270/R744 ($T_e = -45$ºC, $T_c = 50$ºC, $\eta_{comp_{ltc,\,htc}} = 0.8$)

approach is responsible for reduction in maximum COP and maximum exergetic efficiencies for both pairs of refrigerants. The increase in approach is responsible for increase in mass flow rates in 'ltc' and 'htc'. This increase in mass flow rates causes the compressor power requirements to increase in 'ltc' and 'htc'. The increase in total power requirement is responsible for reduction of

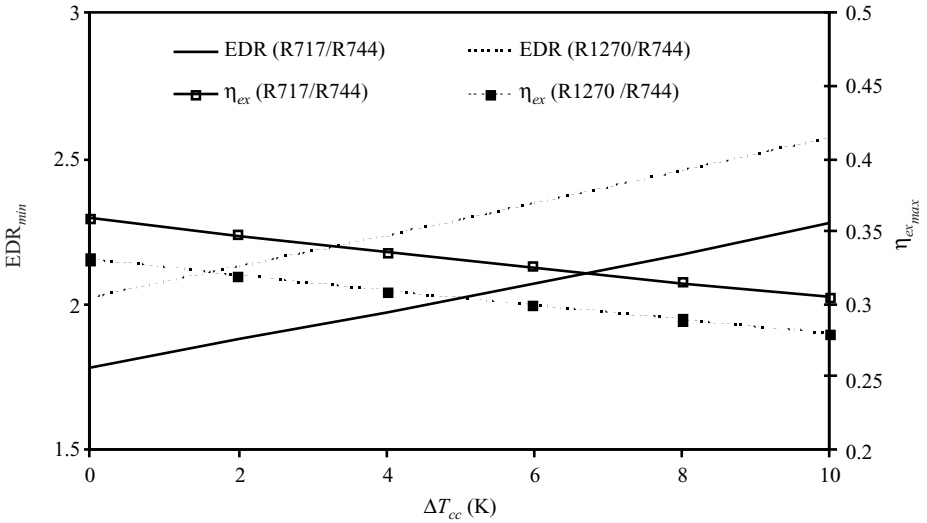

Fig. 2.36 Variation of Minimum EDR and Maximum Exergetic Efficiency with Approach in Cascade Condenser for R717/ R744 and R1270/R744 ($T_e = -45$°C, $T_c = 50$°C, $\eta_{comp_{ltc,\ htc}} = 0.8$)

maximum COP. Simultaneously increase in approach is accountable for increase in exergy destruction due to increase in finite temperature difference in cascade condenser and hence net exergy in product goes down whereas input exergy (total power required for compression) increases. The combined effect of these two factors leads to reduction in exergetic efficiency. The reduction in maximum COP is about 0.021/K (1.5%/K) increase in approach. The decrease in maximum exergetic efficiency is 0.005/K (1.5%/K) rise in approach. The maximum COP and maximum exergetic efficiency for R717/R744 is 7.9 to 8.2% higher (corresponding to 0 K/10 K approach) in comparison to R1270/R744.

Effect of Sub-cooling of Refrigerant in Condenser in 'htc' (ΔT_{sb}) and Superheating of Refrigerant in Evaporator in 'ltc'(ΔT_{sh})

Figures 2.37, 2.38 and 2.39 represent the effect of sub-cooling of refrigerant in condenser in 'htc' and superheating of refrigerant in evaporator in 'ltc' on optimum temperature in cascade condenser, maximum COP and maximum exergetic efficiency for R717/R744. It is observed that the optimum temperature in cascade condenser is highest for the case when both sub-cooling and superheating are neglected. The sub-cooling of refrigerant by 5 K reduces optimum cascade condenser temperature by approximately 1 K. Consequently maximum COP and maximum exergetic efficiency increase by 1.8% approximately.

The increase in maximum COP is achieved because sub-cooling brings about a reduction in mass flow rate in 'htc' and accordingly the power required to operate 'htc' compressor reduces and hence increase in maximum COP is observed. This reduction in power required in 'htc' compressor translates into rise of exergetic efficiency. The superheating of saturated vapour by 5 K in evaporator reduces the optimum cascade condenser temperature by 0.38 K. This causes the mass flow rate in low temperature cycle and pressure ratio across 'ltc' compressor to reduce. The combined effect

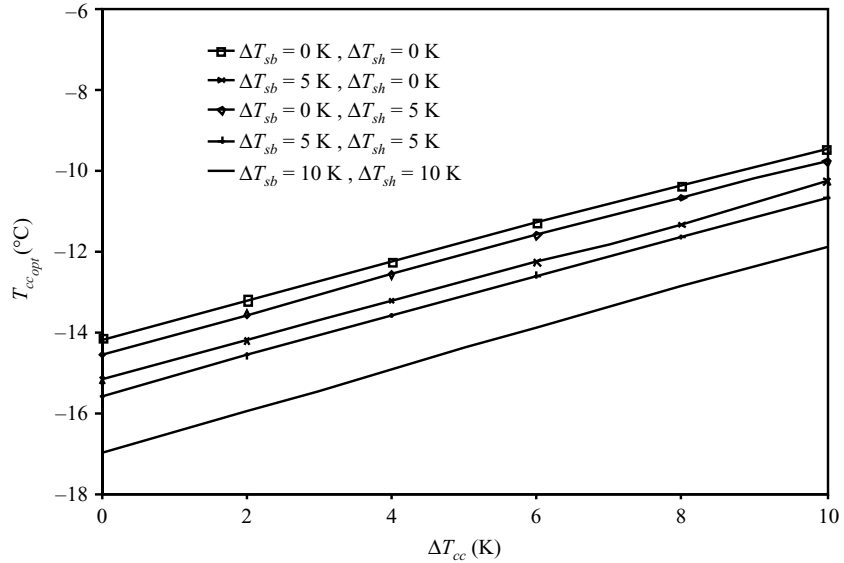

Fig. 2.37 Effect of Approach, Sub-cooling and Superheating on Optimum Temperature in Cascade Condenser for R717/ R744 (T_c = 50°C, T_e = – 45°C, $T_r = T_e$ + 10°C, $\eta_{comp_{ltc,\,htc}}$ = 0.8)

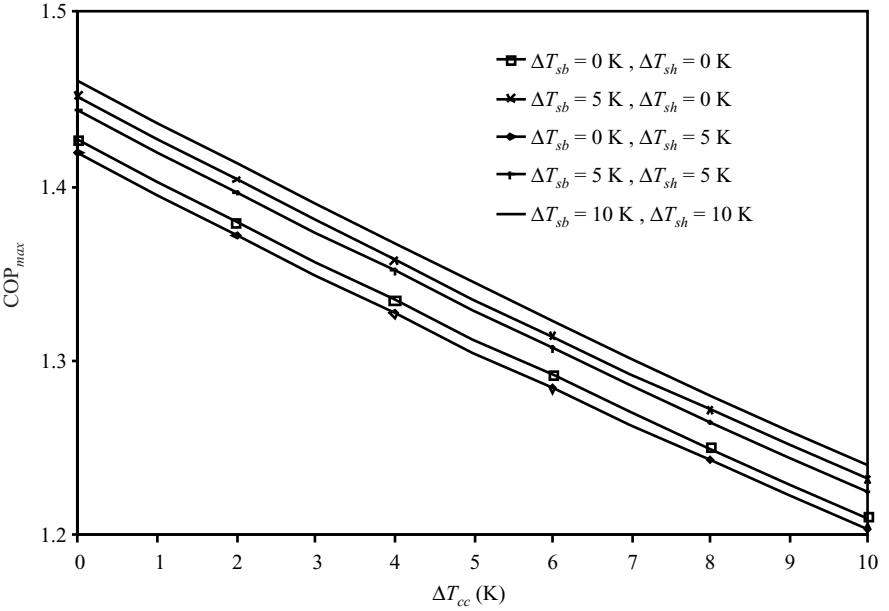

Fig. 2.38 Effect of Approach, Sub-cooling and Superheating on COP_{max} for R717/ R744 (T_c = 50°C, T_e = – 45°C, $T_r = T_e$ + 10°C, $\eta_{comp_{ltc,\,htc}}$ = 0.8)

of these two factors is to decrease the power required in 'ltc' compressor. However, lowering of optimum temperature (and consequently the pressure ratio in 'ltc') accounts for an increase in pressure ratio in 'htc' and as a result the power required by the 'htc' compressor increases. The

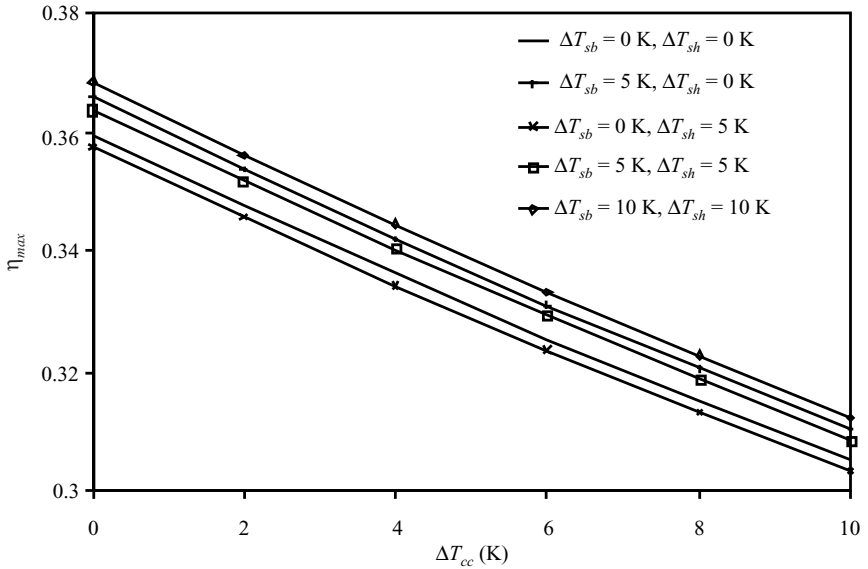

Fig. 2.39 Effect of Approach, Sub-cooling and Superheating on Maximum Exergetic Efficiency for R717/ R744 (T_c = 50°C, T_e = – 45°C, $T_r = T_e$ + 10°C, $\eta_{comp_{ltc,\,htc}}$ = 0.8)

overall effect is increase in the total power required and this reduces maximum COP and maximum exergetic efficiency. The drop in maximum COP and maximum exergetic efficiency is about 0.5%.

Further the combined effect of both sub-cooling and superheating (by 5 K and 10 K) is also illustrated in these figures. It is observed that the combined effect of these factors is to reduce the optimum cascade condenser temperature. In this case reduction in optimum cascade condenser temperature is higher in comparison to case when either sub-cooling or superheating is considered to occur in the system. The combined effect of these two factors (for 5 K) is to increase the maximum COP. However the increase in maximum COP is little less in comparison to the case when sub-cooling (of 5 K) alone was considered. However, the combined effect of these factors (for 10 K) is to increase the maximum COP more than each of the previous case assumed. Similar results are obtained for maximum exergetic efficiency and the same is illustrated in Fig. 2.39.

The effect of sub-cooling and superheating on optimum cascade condenser temperature, maximum COP and maximum exergetic efficiency for R1270/R744 pair is illustrated in Figs. 2.40, 2.41 and 2.42 respectively. It is observed that the trends of results obtained for R1270/R744 is similar to results obtained for R717/R744. In this case, the optimum temperature reduces by 2.7 K for a sub-cooling of 5 K whereas a reduction of only 0.23 K is observed for superheating by 5 K. The increase in maximum COP is about 4.2% for 5 K sub-cooling whereas drop in maximum COP is by 0.55% for superheating by 5 K alone. This shows that the effect of sub-cooling on maximum COP is more in comparison to superheating. Similar to maximum COP, maximum exergetic efficiency also follows the analogous trend; it increases by 4.2% for sub-cooling by 5 K and reduces by about 0.6% for superheating in evaporator by 5 K. The explanation of trends of results is specified already in the previous section. Further the combined effect of these two factors shows that maximum COP and maximum exergetic efficiency increase by about 3.6% for 5 K sub-cooling and 5 K

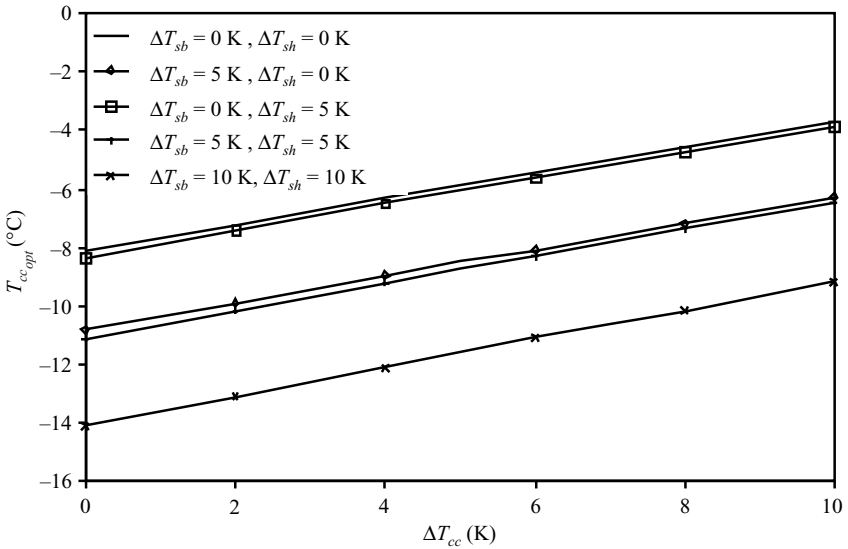

Fig. 2.40 Effect of Variation in Approach, Sub-cooling and Superheating on Optimum Temperature in Cascade Condenser for R1270/R744 (T_e = – 45°C, T_c = 50 °C, $T_r = T_e$ + 10°C, $\eta_{comp_{ltc,\,htc}}$ = 0.8)

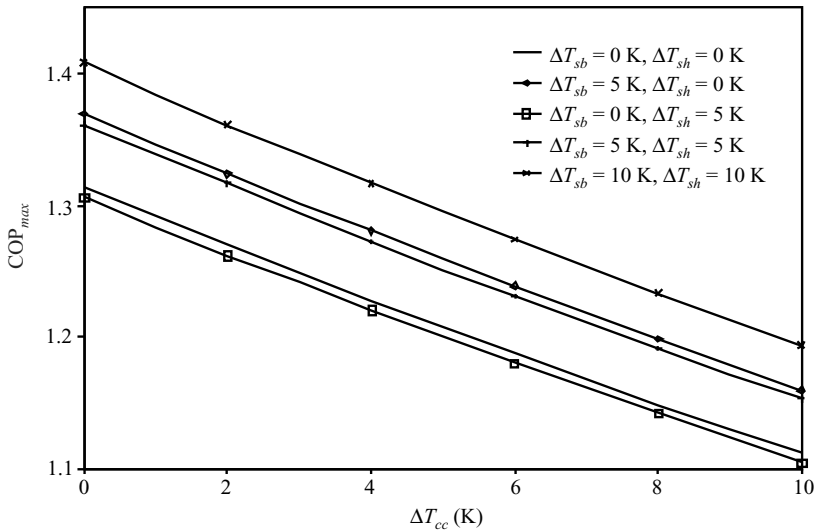

Fig. 2.41 Effect of Variation in Approach, Sub-cooling and Superheating on COP_{max} for R1270/R744 (T_e = – 45°C, T_c = 50°C, $T_r = T_e$ + 10°C, $\eta_{comp_{ltc,\,htc}}$ = 0.8)

superheating whereas the corresponding increase in the values of maximum COP and maximum exergetic efficiency is 7.2% for 10 K sub-cooling and superheating.

Table 2.14 shows comparison of effects of sub-cooling and superheating for R717/R744 and R1270/R744. The difference in values of COP_{max} and $\eta_{ex_{max}}$ for the two pairs shows that sub-cooling is more effective for R1270/R744 as compared to R717/R744.

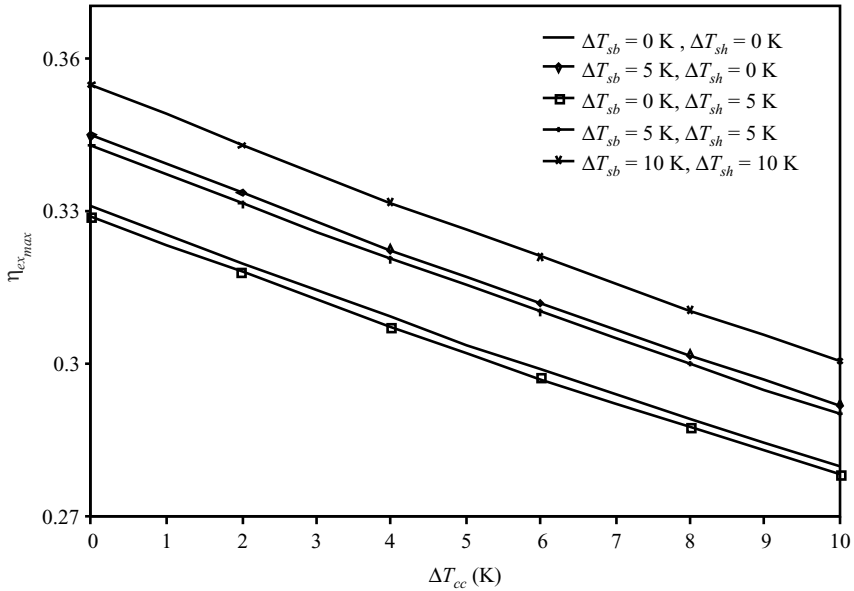

Fig. 2.42 Effect of Variation in Approach, Sub-cooling and Superheating on Maximum Exergetic Efficiency for R1270/R744 (T_e = – 45°C, T_c = 50°C, $T_r = T_e$ + 10°C, $\eta_{comp_{ltc,\ htc}}$ = 0.8)

Table 2.14 Comparison of Effect of Sub-cooling and Superheating on Maximum COP and Maximum Exergetic Efficiency for R717/R744 and R1270/R744 (T_e = – 45°C, T_c = 50°C, $T_r = T_e$ + 10°C, $\eta_{comp_{ltc,\ htc}}$ = 0.8, ΔT_{cc} = 4°C)

ΔT_{sb} (K)	ΔT_{sh} (K)	COP_{max}			$\eta_{ex_{max}}$		
		R717/R744 (a)	**R1270/R744 (b)**	**Difference (a-b)/a**	**R717/R744 (c)**	**R1270/R744 (d)**	**Difference (c-d)/c**
0	0	1.335	1.227	0.0809	0.3363	0.3092	0.08058
5	0	1.358 (1.74%)*	1.28 (4.3%)*	0.05744	0.3422 (1.75%)¥	0.3224 (4.27%)¥	0.05786
0	5	1.327 (– 0.57%)*	1.22 (– 0.6%)*	0.08063	0.3344 (– 0.57%)¥	0.3074 (– 0.58%)¥	0.08074
5	5	1.351 (1.22%)*	1.272 (3.64%)*	0.05848	0.3403 (1.19%)¥	0.3205 (3.65%)¥	0.05818
10	10	1.367 (2.42%)*	1.316 (7.23%)*	0.03731	0.3444 (2.41%)¥	0.3317 (7.28%)¥	0.03688

**The values in percentage in columns (a) and (c) represent the percentage increase or decrease in* COP_{max} *corresponding to the base value of 0 K sub-cooling and 0 K superheating.*

¥Similarly, values in percentage in columns (b) and (d) represent the percentage increase or decrease in $\eta_{ex_{max}}$ *corresponding to the base value of 0 K sub-cooling and 0 K superheating.*

Figure 2.43 shows the efficiency defects in components of cascade refrigeration system for R717/R744 and R1270/R744. It is evident from figure that for R717/R744 efficiency defect in condenser is highest followed by compressor in 'htc', evaporator, refrigerant throttle valve of 'htc', cascade condenser, 'ltc' compressor and 'ltc' refrigerant throttle valve. For R1270/R744, the

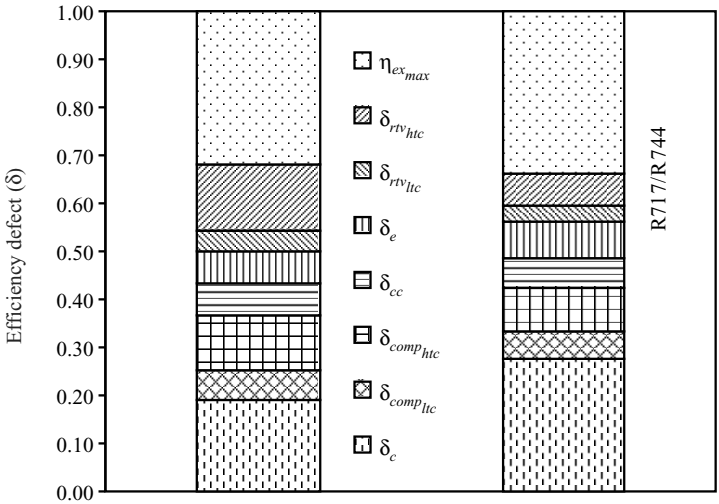

Fig. 2.43 Efficiency Defects in Components of a Cascade Refrigeration System for R717/R744 and R1270/R744 at Optimum Cascade Condenser Temperature
(ΔT_{cc} = 4 K, T_e = – 45ºC, T_c = 50ºC, $T_r = T_e$ + 10ºC, ΔT_{sb} = 5 K, ΔT_{sh} = 5 K, $\eta_{comp_{ltc,\,htc}}$ = 0.8)

efficiency defect is highest in condenser followed by throttle valve, compressor of 'htc', evaporator, cascade condenser, 'ltc' compressor and throttle valve of 'ltc'.

2.5 CONCLUSION

In this chapter the focus has been given on alternative refrigerants and energy and exergy analysis of single stage, multi-compression and cascade vapour compression refrigeration systems. The importance of factors related to environmental and ecological concerns such as ODP, GWP, TEWI and LCCP has been discussed. Various alternative refrigerants such as azeotropes, zeotropes and pure refrigerants as substitutes to conventional refrigerants for different applications have been specified. The chapter also gives the description of Lorenz cycle when using zeotrope refrigerants. It is a modified form of vapour compression cycle in which the boiling and condensation occurs with temperature glide. Another cycle with alternative refrigerant carbon dioxide is transcritical compression refrigeration cycle (used when the critical temperature of refrigerant is low) is also presented. Subsequently, the focus of the chapter shifts to the description and energy and exergy analysis of vapour compression cycle, multistage vapour compression refrigeration cycles and cascade refrigeration cycle. The parametric study of these systems have been carried out under various operating conditions of the systems. In two-stage system, the optimum reduced inter-stage temperatures and pressures have been computed for HCFC 22, R410A and R717, and the value is found very near to saturation pressure corresponding to Geometric Mean Temperature (GMT) of condensation and evaporation temperatures. In cascade refrigeration system two pairs of refrigerants, viz., R717/R744 and R1270/R744 have been considered and optimum cascade condenser temperature has been computed corresponding to maximum exergetic efficiency. The effects of evaporator and condenser temperatures, approach degree of sub-cooling and super-heating have also been highlighted on optimum cascade condenser temperature, COP and exergetic efficiency of the system.

REFERENCES

Agnew, B. and Ameli, S.M., 2004. A finite time analysis of a cascade refrigeration system using alternative refrigerants. *Applied Thermal Engineering* (24), 2557-2565.

Aprea, C., Mastrullo, R. Renno, C. 2004. An analysis of the performances of a vapour compression plant working both as a water chiller and a heat pump using R22 and R417A. *Applied Thermal Engineering* 24, 487-499.

Aprea, C., Mastrullo R., Rossi F. D., 1996. Behaviour and performances of R502 alternative working fluids in refrigerating plants. *International Journal of Refrigeration* 19(4), 257-63.

Arcaklioglu, E., Cavusoglu , A., Erisen A., 2005. An algorithmic approach towards finding better refrigerant substitutes of CFCs in terms of the second law of thermodynamics. *Energy Conversion and Management* 46, 1595-1611.

Arora, C.P., and Dhar, P.L., 1973. Optimization of Multistage refrigerant compressor, Progress in Refrigeration Science and Technology, *XIII International Congress of Refrigeration (IIR).* 693-700.

Arora, A., 2009, Energy and Exegy analysis of compression, absorption and combined cycle cooling systems, Ph.D. Thesis, IIT, Delhi.

Arora, A., Arora, B.B., Pathak B.D. and Sachdev H. L., 2007. Exergy analysis of a Vapour Compression Refrigeration System with R-22, R-407C and R-410A, *International Journal of Exergy* 4(4), 441-454.

ASHRAE Handbook (Fundamentals), 1997, Chapter 18.

Bansal, P. K. and Jain, S., 2007. Cascade systems: past, present, and future. *ASHRAE Transactions* 113(1), 245-252.

Baumnann, K., Blass, E., 1961. Beitrag zur Ermittlung des optimalen Mitteldruckes bei zweistuflgen Kaltdampf Verdichter-Kältemaschinen, Kältetechnik 13, 210-216.

Bejan, A., Tsatsaronis, G., Moran, M., 1996. Thermal Design and Optimization. John Wiley and Sons, USA, pp. 143-156.

Bhattacharyya, S., Mukhopadhyay, S., Kumar A., Khurana R.K. and Sarkar J., 2005. Optimization of a CO2/C3H8 cascade system for refrigeration and heating. *International Journal of Refrigeration* 28, 1284-1292.

Bitzer International: Refrigerant report no. 14 (Edition A-501-14), (http://www.bitzer.de/en/etc/download.php?d=doc/a/&f=a-501-14.pdf, 2007).

Bitzer International: Refrigerant report no. 16 (Edition A-501-16) (http://www.bitzer.de/en/etc/download.php?d=doc/a/&f=a-501-16.pdf).

Bivens and Yokozeki, 1996. International Conference on Ozone Protection Technologies, Washington, DC.

Calm, J. M., 2008. The next generation of refrigerants - Historical review, considerations, and outlook. *International Journal of Refrigeration.* 1-11 (In Press).

Calm J.M., Hourahan G.C., 2001. Refrigerant data summary, Engineered Systems 18, 74-78.

Camporese R., Bigolaro G., Bobbo S. and Cortella, G., 1997. Experimental evaluation of refrigerant mixtures as substitutes for CFC12 and R502. *International Journal of Refrigeration*, 20(1), 22-31.

Chen, W., 2008. A comparative study on the performance and environmental characteristics of R410A and R22 residential air conditioners. *Applied Thermal Engineering* 28, 1-7.

Dopazo J.A., Fernández-Seara J., Sieres J., Uhía F. J., 2009. Theoretical analysis of a CO_2-NH_3 cascade refrigeration system for cooling applications at low temperatures. *Applied Thermal Engineering*, 29(8-9), 1577-1583.

Döring R., Buchwald H. and Hellmann, J., 1997. Results of experimental and theoretical studies of the azeotropic refrigerant R507. *International Journal of Refrigeration*, 20(2), 78-84.

Getu, H.M., Bansal P.K. , 2008. Thermodynamic analysis of an R744-R717 cascade refrigeration system. *International Journal of Refrigeration* 31(1), 45-54.

Göktun S., 1998. An overview of ozone safe alternatives for R502. Energy 23(5), 379-81.

Ratts, E.B. and Brown J.S., 2000. A generalized analysis for cascading single fluid vapour compression refrigeration cycles using an entropy generation minimization method. *International Journal of Refrigeration* 23, 353-365.

Riffat, S. B., Afonso C. F., Oliveirat A. C. and Reay D. A., 1997. Natural refrigerants for refrigeration and Air conditioning systems. *Applied Thermal Engineering* 17(I), 33-42.

Said, S.A. and Ismail, B. 1994. Exergetic assessment of the coolants HCFC123, HFC134a, CFC11 and CFC12. *Energy* 19(11), 1181-86.

Sami, S. M. and Desjardins, D. E., 2000a. Performance and comparative study of new alternatives to R502 inside air/refrigerant enhanced surface tubing. *International Journal of Energy Research* 24 (2), 177-186.

Sami, S. M. and Desjardins, D. E., 2000b. Performance enhancement of some alternatives to R502', *International Journal of Energy Research* 24(4), 279-89.

Sencan, A., Yakut, K.A., Kalogirou, S.A., 2005. Exergy analysis of lithium bromide/water absorption systems. *Renewable Energy* 30, 645-657.

Siller, D.A., Anderson K., Shepherd J. J., Strong R., John R., Vallort R. P., Seaton W.W., 2006 Ammonia as a refrigerant. American Society of Heating, Refrigerating and Air-Conditioning Engineers, Inc.www.ashrae.org/content/ASHRAE/ASHRAE/Article AltFormat/200622793710_347.pdf)

Singh, P. 2009. Study of vortex tube integrated alternative refrigeration and air-conditioning options for energy conservation, Ph.D. Thesis, IIT, Delhi.

Stegou-Sagia A. , Paignigiannis N., 2005. Evaluation of mixtures efficiency in refrigerating systems. *Energy Conversion and Management* 46, 2787-2802.

Threlkeld, J. L.1966. *Thermal Environmental Engineering*, Prentice-Hall, NJ.

Wang, R.Z.and Li Y., 2007. Perspectives for natural working fluids in China, *International Journal of Refrigeration*. 30, 568-581.

Xuan, Y., Chen, G., 2005. Experimental study on HFC-161 mixture as an alternative refrigerant to R502. *International Journal of Refrigeration* 28 (3), 436-441.

Zubair, S. M., Khan, S. H., 1995. On optimum inter-stage pressure for two-stage and mechanical-subcooling vapour-compression refrigeration cycles. ASME Transactions, *Journal of Solar Energy Engineering* 117 (1), 64-66.

Zubair, S. M., Shaw, D. N., 1986. An Experimental Investigation of Two-Stage Refrigeration Systems, Internal Report, Copeland Corporation, Sidney, OH .

Zubair, S.M., Yaqub, M. and Khan, S.H., 1996. Second-law-based thermodynamic analysis of two-stage and mechanical-sub-cooling refrigeration cycles. *International Journal of Refrigeration* 19(8), 506-516.